Identification of Nuclear Localization Signal on *O*-GlcNAc Transferase and Its Nuclear Import Regulation

Hyeon Gyu Seo

The Graduate School
Yonsei University
Department of Integrated OMICS
for Biomedical Science

Identification of Nuclear Localization Signal on *O*-GlcNAc Transferase and Its Nuclear Import Regulation

A Dissertation
Submitted to the Department of Integrated OMICS
for Biomedical Science
and the Graduate School of Yonsei University
in partial fulfillment of the
requirements for the degree of
Doctor of Philosophy

Hyeon Gyu Seo

December 2016

This certifies that the dissertation
of Hyeon Gyu Seo is approved.

_____
Thesis Supervisor: Jin Won Cho

_____
Tae Ho Lee

_____
In Kwon Chung

_____
Nam-on Ku

_____
Jihyun F. Kim

The Graduate School
Yonsei University
December 2016

Table of Contents

List of Figures and Tables

Abbreviations

O-GlcNAc: *O*-linked β-*N*-acetylglucosamine

OGT: *O*-GlcNAc transferase

OGA: *O*-GlcNAcase

UDP-GlcNAc: uridine 5′-diphospho-*N*-acetylglucosamin

TPR: tetratricopeptide repeats

NLS: nuclear localization signal

Thiamet-G:(3aR,5R,6S,7R,7aR)-2-(Ethylamino)-3a,6,7,7a-tetrahydro-5-(hydroxymethyl)-5H-pyrano[3,2-d]thiazole-6,7-diol

5-thio-GlcNAc: uridine diphospho-5-thio-*N*-acetylglucosamine

MEF2C: Myocyte-specific enhancer factor 2C

ADARB1: double-stranded RNA-specific editase 1

XIAP: X-linked inhibitor of apoptosis protein

sWGA: succinylated wheat germ agglutinin

Q-TOF MS: quadrupole time-of-flight tandem mass spectrometry

HeLa: cervical cancer cells

HEK293: Human embryonic kidney cells

HCT116: human colorectal carcinoma cells

A549: adenocarcinomic human alveolar basal epithelial cells

MDA-MB-231: human breast adenocarcinoma cells

Summary

The hexosamine biosynthetic pathway (HBP) is dependent on metabolic nutrients status including glucose, glutamine, and acetyl-CoA. Increased HBP flux leads to upraised post-translational modification of *O*-linked *N*-acetylglucosamine (*O*-GlcNAc) to numerous nuclear and cytoplasmic proteins. This modification is caused by the enzymatic attachment of the *N*-acetylglucosamine (GlcNAc) moiety to the hydroxyl groups of serine or threonines. *O*-GlcNAcylation is dynamically regulated by *O*-GlcNAc transferase (OGT) and *O*-GlcNAcase (OGA), which are responsible for *O*-GlcNAc addition and removal respectively.

The diverse subcellular localization of OGT further affects its interactions with the nuclear or cytoplasmic *O*-GlcNAc modified proteins. Although there are a few reports that OGT is redistributed from the nuclear compartment to the cytosol and plasma membrane, the mechanisms which modulate nuclear import and export of OGT are not well understood. Here, we identified a sequence of three amino acids (DFP) in OGT that play a role as a NLS. Moreover, we revealed that nuclear import of OGT is mediated by importin α5. We also elucidated that *O*-GlcNAcylation of the tetratricopeptide repeats (TPR) domain of OGT is required for its direct nuclear translocation. Overall, our data suggest that both the NLS and *O*-GlcNAc modification of OGT are required for its nuclear localization.

Cancer cells has a general characteristic of abnormally up-regulated total *O*-GlcNAcylation and OGT protein levels. A number of studies suggest that *O*-GlcNAcylation is a central mediator of nutrient status to control important metabolic and signaling pathways that regulate varied cancer cell phenotypes. Although OGT protein level is maintained at a high status, little is known about the mechanisms of OGT protein regulation in cancer cells. Here, we report that X-linked inhibitor

apoptosis protein (XIAP) functions as an E3 ligase and promotes the proteasome-dependent degradation of OGT in vitro and in vivo. XIAP also might be *O*-GlcNAcylated at Ser406 *O*-GlcNAcylated and the modification of XIAP influences on it E3 ligase activity for OGT. The human colorectal carcinoma cells (HCT116) stably overexpressing XIAP showed reduced cell proliferations. Our study demonstrates that a novel function of XIAP in the regulation of cancer cell growth, which is distinctly different from its well characterized anti-apoptotic properties.

Key words: *O*-GlcNAc, *O*-GlcNAc transferase (OGT), nuclear localization signal (NLS), importin α5, tetratricopeptide repaeats (TPR), Cancer cells, X-linked inhibitor apoptosis protein (XIAP), E3 ligase, ubiquitylation, proteasome degradation

Chapter 1

Nucleocytoplasmic *O*-GlcNAc Transferase

1. Abstract

O-GlcNAc transferase (OGT) catalyze the reversible and dynamic cycling of subcellular, post-translational modification on numerous serine or threonine residues of cytoplasmic, nuclear, and mitochondrial signaling proteins. A functionally diverse set of substrate proteins of OGT has been identified, and the extent of *O*-GlcNAcylation fluctuates in response to nutrients and cellular signaling. OGT is implicated in widespread, nutrient-sensing regulation of various signaling pathways and transcriptional programs. Recent studies have also implicated OGT as a regulators of many cancer phenotypes including cancer cell growth, survival, metastasis, angiogenesis and even cancer epigenome. While an emerging interest in the field of *O*-GlcNAc has contributed to understanding the functional impacts of *O*-GlcNAcylated proteins, little is known about the upstream mechanisms which modulate OGT's subcellular localization, post-translational modification, degradation and substrate targeting.

2. OGT's structure and function

O-GlcNAc transferase (OGT) is expressed in all mammalian tissues and is most abundant in brain, heart, pancreas, skeletal muscle, and uterus (Lubas et al., 1997; Nolte and Muller, 2002). OGT gene (~43 kb) residues are highly conserved, present as a single X-linked gene localized at the chromosome Xq13.1, and alternatively spliced to generate nucleocytoplasmic (nc), mitochondrial (m), and short (s) isoforms (Kreppel et al., 1997; Wrabl and Grishin, 2001; Blatch and Lassle, 1999). These OGT isoforms are distinguished by their N-terminal domains which contain a variable number of tetratricopeptide repeats (TPRs), which are common protein-protein interaction domains. The full length ncOGT isoform possesses 13.5 TPRs while mOGT and sOGT isoforms contain 9 and 3 TPRs, respectively (Hanover et al., 2003; Love et al., 2003). mOGT has an additional 120 amino acid stretch at the N-terminus identified as the mitochondrial targeting sequence (Love et al., 2003). Three different OGT isoforms consist of two catalytic regions related to the classic GT-B (glycosyltransferase-B) domains, which is located at the C-terminus (Gao, 2010). An exceptional *O*-GlcNAc transferase, extracellular OGT (EOGT) has been identified in Drosophila. EOGT is localized within the ER lumen and is structurally unconnected to ncOGT. EOGT exploits UDP-GlcNAc for the *O*-GlcNAc modification of epidermal growth factor (EGF)-like domains of secreted proteins (Sakaidani et al., 2012; Sakaidani et al., 2012).

The TPR domain of OGT may affect the OGT's selectivity by mediating its oligomerization. Hetero-trimeric OGTs compose two 110 kDa subunits and one 78 kDa subunit (sOGT) which are found in tissues such as kidney, liver, muscle, spleen, and pancreas (Akimoto et al., 1999; Haltiwanger et al., 1992; Kreppel et al., 1997; Marz et al.,

2006). Homo-oligomeric OGTs have been observed and these homo-oligomers are disrupted by truncation of TPRs' 1-6th residues (Kreppel and Hart, 1999) which also reduces the auto-glycosylation of OGT (Lubas and Hanover, 2000). A recent study reveals that the homo-dimerization of OGT is abolished when two conserved residues (Trp198 and Ile201) within the TPR 6-7th interface were mutated, and these same mutations abate the *O*-GlcNAcylation of Nup62 (Jinek et al., 2004).

OGT is also regulated by post-translational modifications. OGT undergoes auto-GlcNAcylation between amino acids 380 and 396 in the 9th TPR and between amino acids 1027 and 1036 in the C-terminal catalytic domain and, and phosphorylation occurs at Thr444 and Tyr969 of OGT (Kreppel et al., 1997; Lubas et al., 2000; Tai et al., 2004). The function of *O*-GlcNAcylation of OGT has not been discovered. One report shows that OGT activity is raised upon increased tyrosine 969 phosphorylation of OGT following insulin treatment in 3T3-L1 adipocytes (Song et al., 2008; Whelan., 2008). However, the specific mechanisms underlying how the phosphorylation sites regulate OGT activity are still not elucidated.

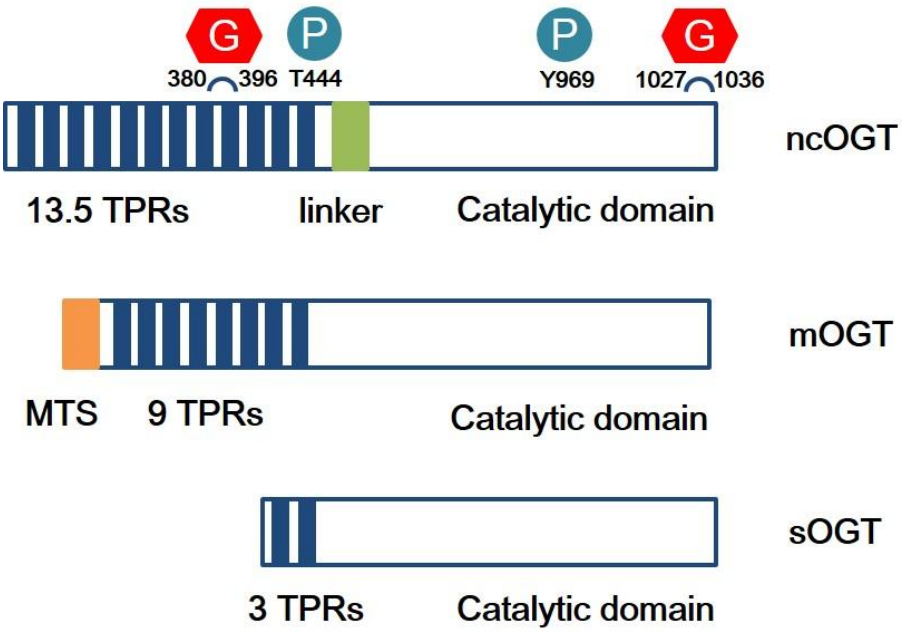

Figure 1. Schematic domain structures of OGT

Human OGT possesses a N-terminal tetratricopeptide repeats (TPRs) and catalytic domain and three isoforms are generated by alternative promoter usage from a single gene which resides in chromosome X. ncOGT contains 13.5 TPRs and is localized predominantly more in the nucleus and less in the cytoplasm. mOGT has mitochondrial targeting sequence (MTS) at the N-terminus. mOGT and sOGT possess 9 TPRs and 3 TPRs, respectively. Reported post-translational modifications of OGT are indicated by amino acid residues.

3. Intracellular localization of OGT

OGT's subcellular localization influences its interaction with other cellular *O*-GlcNAc modified proteins. OGT is localized both in the nucleus and the cytoplasm (Akimoto et al., 1999; Love et al., 2003; Lubas et al., 1997). The localization of OGT can be modulated by transient complex formation with other adopter proteins. OGT forms a complex with *O*-GlcNAcase, mitotic aurora B kinase, and protein phosphatase 1c (PP1c) at the mitotic spindle during mitosis (Slawson et al., 2008). When aurora B kinase activity is inhibited, translocation of OGT to the midbody is abolished during cytokinesis. Another example of OGT's subcellular translocation is that OGT is localized to the transcriptional initiation sites for *O*-GlcNAc modification of RNA polymerase Ⅱ, forming a complex with trafficking kinesin-binding 1 protein (TRAK1), a microtubule-associated protein (Iyer et al., 2003).

These findings that OGT utilizes its interacting partners for OGT localization could explain why there are no canonical substrate sequence motifs for *O*-GlcNAc modification unlike phosphorylation motifs. OGT may interact with specific pools of other proteins in specific signal dependent manners.

4. Regulation of OGT

OGT is known to be regulated by several different mechanisms. The mRNA and protein levels of OGT are oscillated during cell cycle progression (Dehennaut et al., 2007; Drougat et al., 2012; Lefebvre et al., 2004; Slawson et al., 2005; Yang et al., 2012) and are tissue specific (Andres-Bergos et al., 2012; Ogawa et al., 2012). OGT transcription, protein expression, and activity are also affected by numerous stressors, including oxidative, osmotic, thermal, and nutrient availability (Cheung and Hart, 2008; Zachara and Hart, 2004; Zachara et al., 2004), and this is consistent with its acting as a stress modulator and nutrient sensor.

OGT activity is impacted by the available levels of UDP-GlcNAc, a donor substrate. OGT affinity regarding its peptide substrates can be raised by increasing UDP-GlcNAc concentrations (Haltiwanger et al., 1992; Kreppel et al., 1997; Kreppel and Hart, 1999). Recently reports reveal that OGT activity against specific substrate proteins can be regulated through interaction between OGT and its interacting partner proteins, depending on specific signal transduction pathways. During glucose deprivation, OGT interacts with the stress kinase, p38, and activated p38 recruits OGT to specific targets, including neurofilament-H (NF-H). Inhibition of p38 influences OGT activity toward specific target proteins (Cheung and Hart, 2008). Correspondingly, substrate specificity of OGT is changed in the expression of a myosine phosphatase targeting protein (MYPT1), or a co-activator associated arginine methyltransferase 1 (CARM1) (Cheung et al., 2008). Another example of OGT activity modulation by OGT's interacting proteins is *O*-GlcNAc modified forkhead box protein O1 (FoxO1). Under hyperglycemic conditions, the transcription coactivator, Peroxisome proliferator-activated receptor gamma coactivator 1-alpha (PGC-1α), binds to OGT and promotes OGT activity regarding the

transcription factor FoxO1 (Housley et al., 2008; Housley et al., 2009).

5. Future directions

O-GlcNAc modification is a fast growing field with nearly over a thousand *O*-GlcNAcylated proteins identified since its first detection. Many of these *O*-GlcNAc modified proteins are crucial regulatory proteins in cellular signaling pathways, proposing that *O*-GlcNAc modification is one of the major directors in cellular processes and metabolism. Recent studies reveal that improper *O*-GlcNAcylation causes serious effects on cellular metabolism. Cancer cells undergo metabolic re-programing and exhibit abnormal levels of OGT and *O*-GlcNAc modification. However, there is still little investigation of the mechanisms underlying how OGT is regulated in subcellular localization or expressed at high levels in many different types of cancer. Further studies on OGT regulations will provide a better understanding of the roles in *O*-GlcNAc dependent modulation of signaling pathways involved in metabolic re-programing of cancer. Therapeutic window may exist to pointedly target OGT in cancer cells.

Cancer	OGT and *O*-GlcNAc
Breast	Elevated OGT/*O*-GlcNAc in cancer cells and OGT RNA elevated in invasive breast cancer *O*-GlcNAcylation/OGT increased in primary malignant tumors compared to benign tumors
Prostate	Elevated OGT/*O*-GlcNAc in cancer cells; OGT increase associated with progression and poor survival
Colon	*O*-GlcNAcylation, OGT elevated in colon cancer tissue compared to adjacent tissue; Metastatic CRC cell clones contain increased *O*-GlcNAcylation compared to primary clones
Lung	*O*-GlcNAcylation and OGT levels are elevated in lung squamous cell carcinoma tissue compared to adjacent lung tissue; PFK-1 is hyper-*O*-GlcNAcylated in cancers
Liver	*O*-GlcNAcylation elevated in hepatocellular carcinoma compared to healthy liver; *O*-GlcNAcylation elevated in recurrent HCC patients
Bladder	OGT transcript levels are significantly higher in grade II and III in comparison to grade I bladder cancer; significant increase in OGT expression between early bladder cancers and invasive or advanced bladder cancers
Pancreatic	Elevated *O*-GlcNAcylation, OGT and decreased OGA found in human pancreatic cancer cell lines compared to non-tumorigenic pancreatic epithelial cells
Leukemia	Chronic lymphocytic leukemia patients contain elevated *O*-GlcNAcylation compared to normal circulating B cells. Mouse model of T-cell acute lymphoblastic leukemia requires OGT.

Table 1. Abnormal regulation of OGT and *O*-GlcNAcylation in cancer

6. References

Akimoto, Y., Hart, G.W., Wells, L., Vosseller, K., Yamamoto, K., Munetomo, E., Ohara-Imaizumi, M., Nishiwaki, C., Nagamatsu, S., Hirano, H., et al. (2007). Elevation of the post-translational modification of proteins by O-linked N-acetylglucosamine leads to deterioration of the glucose-stimulated insulin secretion in the pancreas of diabetic Goto-Kakizaki rats. Glycobiology 17, 127-140.

Akimoto, Y., Kreppel, L.K., Hirano, H., and Hart, G.W. (1999). Localization of the O-linked N-acetylglucosamine transferase in rat pancreas. Diabetes 48, 2407-2413.

Andres-Bergos, J., Tardio, L., Larranaga-Vera, A., Gomez, R., Herrero-Beaumont, G., and Largo, R. (2012). The increase in O-linked N-acetylglucosamine protein modification stimulates chondrogenic differentiation both in vitro and in vivo. J Biol Chem 287, 33615-33628.

Blatch, G.L., and Lassle, M. (1999). The tetratricopeptide repeat: a structural motif mediating protein-protein interactions. Bioessays 21, 932-939.

Bullen, J.W., Balsbaugh, J.L., Chanda, D., Shabanowitz, J., Hunt, D.F., Neumann, D., and Hart, G.W. (2014). Cross-talk between two essential nutrient-sensitive enzymes: O-GlcNAc transferase (OGT) and AMP-activated protein kinase (AMPK). J Biol Chem 289, 10592-10606.

Butkinaree, C., Park, K., and Hart, G.W. (2010). O-linked beta-N-acetylglucosamine (O-GlcNAc): Extensive crosstalk with phosphorylation to regulate signaling and transcription in response to nutrients and stress. Biochim Biophys Acta 1800, 96-106.

Caldwell, S.A., Jackson, S.R., Shahriari, K.S., Lynch, T.P., Sethi, G.,

Walker, S., Vosseller, K., and Reginato, M.J. (2010). Nutrient sensor O-GlcNAc transferase regulates breast cancer tumorigenesis through targeting of the oncogenic transcription factor FoxM1. Oncogene 29, 2831-2842.

Champattanachai, V., Netsirisawan, P., Chaiyawat, P., Phueaouan, T., Charoenwattanasatien, R., Chokchaichamnankit, D., Punyarit, P., Srisomsap, C., and Svasti, J. (2013). Proteomic analysis and abrogated expression of O-GlcNAcylated proteins associated with primary breast cancer. Proteomics 13, 2088-2099.

Cheung, W.D., and Hart, G.W. (2008). AMP-activated protein kinase and p38 MAPK activate O-GlcNAcylation of neuronal proteins during glucose deprivation. J Biol Chem 283, 13009-13020.

Cheung, W.D., Sakabe, K., Housley, M.P., Dias, W.B., and Hart, G.W. (2008). O-linked beta-N-acetylglucosaminyltransferase substrate specificity is regulated by myosin phosphatase targeting and other interacting proteins. J Biol Chem 283, 33935-33941.

Dehennaut, V., Lefebvre, T., Sellier, C., Leroy, Y., Gross, B., Walker, S., Cacan, R., Michalski, J.C., Vilain, J.P., and Bodart, J.F. (2007). O-linked N-acetylglucosaminyltransferase inhibition prevents G2/M transition in Xenopus laevis oocytes. J Biol Chem 282, 12527-12536.

Dehennaut, V., Slomianny, M.C., Page, A., Vercoutter-Edouart, A.S., Jessus, C., Michalski, J.C., Vilain, J.P., Bodart, J.F., and Lefebvre, T. (2008). Identification of structural and functional O-linked N-acetylglucosamine-bearing proteins in Xenopus laevis oocyte. Mol Cell Proteomics 7, 2229-2245.

Drougat, L., Olivier-Van Stichelen, S., Mortuaire, M., Foulquier, F., Lacoste, A.S., Michalski, J.C., Lefebvre, T., and Vercoutter-Edouart,

A.S. (2012). Characterization of O-GlcNAc cycling and proteomic identification of differentially O-GlcNAcylated proteins during G1/S transition. Biochim Biophys Acta 1820, 1839-1848.

Ferrer, C.M., Lynch, T.P., Sodi, V.L., Falcone, J.N., Schwab, L.P., Peacock, D.L., Vocadlo, D.J., Seagroves, T.N., and Reginato, M.J. (2014). O-GlcNAcylation regulates cancer metabolism and survival stress signaling via regulation of the HIF-1 pathway. Mol Cell 54, 820-831.

Gu, Y., Gao, J., Han, C., Zhang, X., Liu, H., Ma, L., Sun, X., and Yu, W. (2014). O-GlcNAcylation is increased in prostate cancer tissues and enhances malignancy of prostate cancer cells. Mol Med Rep 10, 897-904.

Gu, Y., Mi, W., Ge, Y., Liu, H., Fan, Q., Han, C., Yang, J., Han, F., Lu, X., and Yu, W. (2010). GlcNAcylation plays an essential role in breast cancer metastasis. Cancer Res 70, 6344-6351.

Haltiwanger, R.S., Blomberg, M.A., and Hart, G.W. (1992). Glycosylation of nuclear and cytoplasmic proteins. Purification and characterization of a uridine diphospho-N-acetylglucosamine:polypeptide-beta-N acetylglucosaminyltransferase. J Biol Chem 267, 9005-9013.

Hanover, J.A., Yu, S., Lubas, W.B., Shin, S.H., Ragano-Caracciola, M., Kochran, J., and Love, D.C. (2003). Mitochondrial and nucleocytoplasmic isoforms of O-linked GlcNAc transferase encoded by a single mammalian gene. Arch Biochem Biophys 409, 287-297.

Housley, M.P., Rodgers, J.T., Udeshi, N.D., Kelly, T.J., Shabanowitz, J., Hunt, D.F., Puigserver, P., and Hart, G.W. (2008). O-GlcNAc regulates FoxO activation in response to glucose. J Biol Chem 283, 16283-16292.

Housley, M.P., Udeshi, N.D., Rodgers, J.T., Shabanowitz, J., Puigserver, P., Hunt, D.F., and Hart, G.W. (2009). A PGC-1alpha-O-GlcNAc transferase complex regulates FoxO transcription factor activity in

response to glucose. J Biol Chem 284, 5148-5157.

Itkonen, H.M., Minner, S., Guldvik, I.J., Sandmann, M.J., Tsourlakis, M.C., Berge, V., Svindland, A., Schlomm, T., and Mills, I.G. (2013). O-GlcNAc transferase integrates metabolic pathways to regulate the stability of c-MYC in human prostate cancer cells. Cancer Res 73, 5277-5287.

Jinek, M., Rehwinkel, J., Lazarus, B.D., Izaurralde, E., Hanover, J.A., and Conti, E. (2004). The superhelical TPR-repeat domain of O-linked GlcNAc transferase exhibits structural similarities to importin alpha. Nat Struct Mol Biol 11, 1001-1007.

Kamigaito, T., Okaneya, T., Kawakubo, M., Shimojo, H., Nishizawa, O., and Nakayama, J. (2014). Overexpression of O-GlcNAc by prostate cancer cells is significantly associated with poor prognosis of patients. Prostate Cancer Prostatic Dis 17, 18-22.

Kreppel, L.K., Blomberg, M.A., and Hart, G.W. (1997). Dynamic glycosylation of nuclear and cytosolic proteins. Cloning and characterization of a unique O-GlcNAc transferase with multiple tetratricopeptide repeats. J Biol Chem 272, 9308-9315.

Kreppel, L.K., and Hart, G.W. (1999). Regulation of a cytosolic and nuclear O-GlcNAc transferase. Role of the tetratricopeptide repeats. J Biol Chem 274, 32015-32022.

Krzeslak, A., Forma, E., Bernaciak, M., Romanowicz, H., and Brys, M. (2012). Gene expression of O-GlcNAc cycling enzymes in human breast cancers. Clin Exp Med 12, 61-65.

Love, D.C., Kochan, J., Cathey, R.L., Shin, S.H., and Hanover, J.A. (2003). Mitochondrial and nucleocytoplasmic targeting of O-linked GlcNAc transferase. J Cell Sci 116, 647-654.

Lubas, W.A., Frank, D.W., Krause, M., and Hanover, J.A. (1997). O-Linked GlcNAc transferase is a conserved nucleocytoplasmic protein containing tetratricopeptide repeats. J Biol Chem 272, 9316-9324.

Lubas, W.A., and Hanover, J.A. (2000). Functional expression of O-linked GlcNAc transferase. Domain structure and substrate specificity. J Biol Chem 275, 10983-10988.

Lynch, T.P., Ferrer, C.M., Jackson, S.R., Shahriari, K.S., Vosseller, K., and Reginato, M.J. (2012). Critical role of O-Linked beta-N-acetylglucosamine transferase in prostate cancer invasion, angiogenesis, and metastasis. J Biol Chem 287, 11070-11081.

Lynch, T.P., and Reginato, M.J. (2011). O-GlcNAc transferase: a sweet new cancer target. Cell Cycle 10, 1712-1713.

Ma, Z., Vocadlo, D.J., and Vosseller, K. (2013). Hyper-O-GlcNAcylation is anti-apoptotic and maintains constitutive NF-kappaB activity in pancreatic cancer cells. J Biol Chem 288, 15121-15130.

Mi, W., Gu, Y., Han, C., Liu, H., Fan, Q., Zhang, X., Cong, Q., and Yu, W. (2011). O-GlcNAcylation is a novel regulator of lung and colon cancer malignancy. Biochim Biophys Acta 1812, 514-519.

Nolte, D., and Muller, U. (2002). Human O-GlcNAc transferase (OGT): genomic structure, analysis of splice variants, fine mapping in Xq13.1. Mamm Genome 13, 62-64.

Ogawa, M., Mizofuchi, H., Kobayashi, Y., Tsuzuki, G., Yamamoto, M., Wada, S., and Kamemura, K. (2012). Terminal differentiation program of skeletal myogenesis is negatively regulated by O-GlcNAc glycosylation. Biochim Biophys Acta 1820, 24-32.

Phueaouan, T., Chaiyawat, P., Netsirisawan, P., Chokchaichamnankit, D.,

Punyarit, P., Srisomsap, C., Svasti, J., and Champattanachai, V. (2013). Aberrant O-GlcNAc-modified proteins expressed in primary colorectal cancer. Oncol Rep 30, 2929-2936.

Sakaidani, Y., Ichiyanagi, N., Saito, C., Nomura, T., Ito, M., Nishio, Y., Nadano, D., Matsuda, T., Furukawa, K., and Okajima, T. (2012). O-linked-N-acetylglucosamine modification of mammalian Notch receptors by an atypical O-GlcNAc transferase Eogt1. Biochem Biophys Res Commun 419, 14-19.

Sakaidani, Y., Nomura, T., Matsuura, A., Ito, M., Suzuki, E., Murakami, K., Nadano, D., Matsuda, T., Furukawa, K., and Okajima, T. (2011). O-linked-N-acetylglucosamine on extracellular protein domains mediates epithelial cell-matrix interactions. Nat Commun 2, 583.

Slawson, C., and Hart, G.W. (2011). O-GlcNAc signalling: implications for cancer cell biology. Nat Rev Cancer 11, 678-684.

Slawson, C., Lakshmanan, T., Knapp, S., and Hart, G.W. (2008). A mitotic GlcNAcylation/phosphorylation signaling complex alters the posttranslational state of the cytoskeletal protein vimentin. Mol Biol Cell 19, 4130-4140.

Tai, H.C., Khidekel, N., Ficarro, S.B., Peters, E.C., and Hsieh-Wilson, L.C. (2004). Parallel identification of O-GlcNAc-modified proteins from cell lysates. J Am Chem Soc 126, 10500-10501.

Wellen, K.E., Lu, C., Mancuso, A., Lemons, J.M., Ryczko, M., Dennis, J.W., Rabinowitz, J.D., Coller, H.A., and Thompson, C.B. (2010). The hexosamine biosynthetic pathway couples growth factor-induced glutamine uptake to glucose metabolism. Genes Dev 24, 2784-2799.

Whelan, S.A., Lane, M.D., and Hart, G.W. (2008). Regulation of the O-linked beta-N-acetylglucosamine transferase by insulin signaling. J

Biol Chem 283, 21411-21417.

Wrabl, J.O., and Grishin, N.V. (2001). Homology between O-linked GlcNAc transferases and proteins of the glycogen phosphorylase superfamily. J Mol Biol 314, 365-374.

Yang, Y.R., Kim, D.H., Seo, Y.K., Park, D., Jang, H.J., Choi, S.Y., Lee, Y.H., Lee, G.H., Nakajima, K., Taniguchi, N., et al. (2015). Elevated O-GlcNAcylation promotes colonic inflammation and tumorigenesis by modulating NF-kappaB signaling. Oncotarget 6, 12529-12542.

Yehezkel, G., Cohen, L., Kliger, A., Manor, E., and Khalaila, I. (2012). O-linked beta-N-acetylglucosaminylation (O-GlcNAcylation) in primary and metastatic colorectal cancer clones and effect of N-acetyl-beta-D-glucosaminidase silencing on cell phenotype and transcriptome. J Biol Chem 287, 28755-28769.

Yi, W., Clark, P.M., Mason, D.E., Keenan, M.C., Hill, C., Goddard, W.A., 3rd, Peters, E.C., Driggers, E.M., and Hsieh-Wilson, L.C. (2012). Phosphofructokinase 1 glycosylation regulates cell growth and metabolism. Science 337, 975-980.

Zachara, N.E., and Hart, G.W. (2004). O-GlcNAc a sensor of cellular state: the role of nucleocytoplasmic glycosylation in modulating cellular function in response to nutrition and stress. Biochim Biophys Acta 1673, 13-28.

Zhu, Q., Zhou, L., Yang, Z., Lai, M., Xie, H., Wu, L., Xing, C., Zhang, F., and Zheng, S. (2012). O-GlcNAcylation plays a role in tumor recurrence of hepatocellular carcinoma following liver transplantation. Med Oncol 29, 985-993.

Chapter 2

Identification of Nuclear Localization Signal of *O*-GlcNAc Transferase and Its Nuclear Import Regulation

1. Abstracts

Nucleocytoplasmic *O*-GlcNAc transferase (OGT) attaches a single GlcNAc to hydroxyl groups of serine and threonine residues. Although the cellular localization of OGT is important to regulate a variety of cellular processes, the molecular mechanisms regulating the nuclear localization of OGT is unclear. Here, we characterized three amino acids (DFP; residues 451 - 453) as the nuclear localization signal of OGT and demonstrated that this motif mediated the nuclear import of non-diffusible β-galactosidase. OGT bound the importin α5 protein, and this association was abolished when the DFP motif of OGT was mutated or deleted. We also revealed that *O*-GlcNAcylation of Ser389, which resides in the tetratricopeptide repeats, plays an important role in the nuclear localization of OGT. Our findings may explain how OGT, which possesses a NLS, exists in the nucleus and cytosol simultaneously.

2. Introduction

O-linked *N*-acetylglucosamine (*O*-GlcNAc) modification occurs on serine or threonine residues of various proteins in the nucleus and cytoplasm, similar to phosphorylation (Wells et al., 2001). Since the discovery of *O*-GlcNAcylation by Hart and Torres in 1984 (Torres and Hart, 1984), *O*-GlcNAc has been implicated in many fundamental biological processes including various signaling pathways, proteasomal degradation, epigenetic regulation, protein-protein interactions, transcription, translation and the stress response (Hanover, 2010; Ozcan et al., 2010; Roos et al., 1997; Ruan et al., 2013; Slawson et al., 2006; Wells et al., 2003). *O*-GlcNAcylation is reversible and highly dynamic, and is controlled by only two enzymes. *O*-GlcNAc transferase (OGT) catalyzes the addition of *O*-GlcNAc and *O*-GlcNAcase removes *O*-GlcNAc (Dong and Hart, 1994; Haltiwanger et al., 1992). *O*-GlcNAc modification interplays with phosphorylation in a reciprocal and competitive manner (Hu et al., 2010). The gene encoding OGT was first described in rat liver and is ubiquitously expressed in higher eukaryotes (Kreppel et al., 1997). In mammals, the three variants of OGT are synthesized by alternative splicing of the amino-terminus tetratricopeptide repeat (TPR) domain. Nucleocytoplasmic OGT contains 13.5 domains and is found in the nucleus and cytoplasm. mOGT, the mitochondrial OGT, has a mitochondrial targeting sequence with nine TPRs, and sOGT, the short form OGT, only contains three TPRs (Hanover et al., 2003; Love et al., 2003; Lubas et al., 1997). The crystal structure of the TPR domain of human OGT is similar to the transport protein importin α and shows the enzyme as a dimer with a large super helix at the inner surface (Jinek et al., 2004). OGT is also comprised of a C-terminal catalytic domain, whose crystal structure indicates there is a pivot point between the twelfth and thirteenth TPR, a flexible region called a hinge that is capable of large motions

(Lazarus et al., 2011). Although there are reports of the subcellular translocation of OGT (Bullen et al., 2014; Whelan et al., 2008), the mechanism underlying how OGT can be both localized in the nucleus and remain in the cytoplasm is obscure.

The transport of proteins between the nucleus and cytoplasm is a highly regulated process. Nuclear import substrates possess nuclear localization signals (NLS), which are recognized by distinct transport factors such as importin αs (Adam et al., 1991; Cortes et al., 1994; Gorlich et al., 1994; Kohler et al., 1997; Kohler et al., 1999; Nachury et al., 1998; Seki et al., 1997; Weis et al., 1995) Importin αs act as adaptors by binding to both the import substrate and importin β. This trimeric import complex docks to the nuclear pore complex through importin β and translocates into the nucleus (Cautain et al., 2015; Gorlich et al., 1995; Xu et al., 2004). The mono- or bipartite motif of NLS is recognized by different members of the importin α family, which is divided into α1, α3, α4, α5, α6 and α7. On the other hand, only one importin β has been described in humans (Goldfarb et al., 2004; Kamei et al,. 1999; Kohler et al., 1997; Kohler et al., 1999; Nachury et al., 1998; Prieve et al., 1998; Tsuji et al., 1997). Although nuclear import via the canonical mechanism is most common, other proteins enter the nucleus independently because of their ability to interact directly with components of nuclear pore complexes (Xu et al., 2003).

Here, we identified a sequence of three amino acids (DFP) in OGT that act as a NLS. Moreover, we revealed that nuclear import of OGT is mediated by importin α5. We also elucidated that *O*-GlcNAcylation of the TPR domain of OGT is required for its direct nuclear translocation. Overall, our data suggest that both the NLS and *O*-GlcNAc modification of OGT are required for its nuclear localization.

3. Materials and Methods

Cell culture, DNA transfection and plasmids

HEK293 and HeLa cells were cultured in Dulbecco's Modified Eagle's Medium (Hyclone, Logan, UT) supplemented with 10% fetal bovine serum, 100 U/ml penicillin and 100 μg/ml streptomycin at 37°C in 5% CO_2. DNA was transfected using polyethylenimine (Sigma-Aldrich, St Louis, MO) as described previously (Boussif et al., 1995). siRNA was transfected by lipofection (Lipofectamine Plus; Invitrogen, Carlsbad, CA). Human WT-OGT, mutant OGT, WT-β-galactosidase and mutant β-galactosidase were cloned into the p3xFLAG-CMV™-7.1 ExpressionVector (Sigma-Aldrich, St Louis, MO). Human importin proteins were cloned into pRK5 in frame with an N-terminal Myc epitope. Human MEF2C was cloned into pEXPR-IBA105 Strep tag vector (IBA, Goettingen, Germany). The OGT mutants with deletion of residues 451 - 453 and substitution of residues 451 - 453 to alanine and β-galactosidase fused to DFP were generated by PCR. The other OGT mutants, including OGT-W198E, I201D (Trp198 mutated to glutamate and Ile201 mutated to aspartate), OGT-S381A (Ser381 mutated to alanine), OGT-T383V (Thr383 mutated to valine), OGT-S389A (Ser389 mutated to alanine) and OGT-T394V (Thr394 mutated to valine), were generated using the QuikChange Site-Directed Mutagenesis Kit (Stratagene, La Jolla, CA). The mutations were confirmed by DNA sequence analysis. To generate GST-tagged importin α5, the cDNA encoding full-length importin α5 was cloned downstream of the GST coding sequence in pGEX-5X (Clontech, Rockville, MD)

Reagent and antibodies

Thiamet-G was kindly provided by Dr Kwan Soo Kim (Yonsei University, Seoul, Korea) and 5-thio-GlcNAc was kindly provided by

David Vocadlo (Simon Fraser University, Canada). Antibodies were used against Flag (F-3156, mouse monoclonal, Sigma-Aldrich, St Louis, MO), Myc (B-14, mouse monoclonal, Santa Cruz, Dallas, Texas), GST (9E10, mouse monoclonal, Santa Cruz), α-tubulin (TU-02, mouse monoclonal, Santa Cruz, Dallas, Texas), β-actin (C-2, mouse monoclonal, Santa Cruz, Dallas, Texas), lamin A/C (#2032, rabbit polyclonal, Cell Signaling, Beverly, MA), MEF2C (#5030, rabbit monoclonal, Cell Signaling, Beverly, MA), OGT (DM17, rabbit polyclonal, Sigma-Aldrich, St Louis, MO) and importin α5 (SAB2500572, goat polyclonal, Sigma-Aldrich, St Louis, MO). CTD110.6, an antibody against *O*-GlcNAc, was purchased from Covance (Princeton, NJ).

Western blotting, immunoprecipitation and GST precipitation

For western blotting, cells were lysed in NET buffer (150 mM NaCl, 1% Nonidet P-40 [NP-40], 50 mM Tris-HCl and 1 mM EDTA, pH 8.0) supplemented with a protease inhibitor cocktail (Roche, Mannheim, Germany) for 30 min on ice. Protein concentrations were determined by the Bio-Rad protein assay (Hercules, CA). Protein samples were subjected to reducing SDS-PAGE and transferred to nitrocellulose membranes (Amersham, Piscataway, NJ). For immunoprecipitation, cell lysates were gently mixed with specific antibodies and protein A/G beads (Santa Cruz, Dallas, Texas) for 4 h at 4°C. Immunoprecipitates were washed three times with lysis buffer, eluted with SDS sample buffer and subjected to reducing SDS-PAGE. For co-immunoprecipitation, cells were lysed in co-immunoprecipitation buffer (50 mM Tris-HCl, pH 7.4; 150 mM NaCl; 0.5% NP-40; 1 mM DTT; 0.1 mM EDTA and a protease inhibitor cocktail) and incubated with Flag antibody-conjugated A/G beads for 3 h at 4°C. Thereafter, the beads were washed three times with co-immunoprecipitation washing buffer (20 mM HEPES, pH 7.4; 2 mM $MgCl_2$; 2mM EGTA; 150 mM NaCl and 0.1% Triton X-100), suspended in sample buffer and

subjected to western blotting. Recombinant GST-importin α5 was purified using Glutathione-Sepharose4B (GE Healthcare), and 5μg of beads containing bound proteins were incubated with pre-cleared cell lysates for 2h at 4°C. The precipitated proteins were washed extensively and subjected to western blot analysis.

Immunofluorescence microscopy

Cells were grown on precision coverslips (0.17 ± 0.01 mM thickness; Glaswarenfabrik Karl Hecht GmbH & Co KG, Sondheim, Germany) and preparation of the cells were described previously (Park et al., 2014). For immunofluorescence analysis, mouse monoclonal anti-Flag antibodies (1:5000) were applied for 2 h, followed by rinses (2 × 5 min) in PBS containing 1% bovine serum albumin and incubation with the appropriate fluorescent secondary antibodies for 1 h. DAPI was used to stain nuclei. After rinsing, coverslips were mounted on glass slides with Mowiol. Immunofluorescence was recorded with a Zeiss LSM 510 confocal microscope (Zeiss, Jena, Germany) using a Plan-Apochromat 63× objective (1.4 NA). Meta Imaging Series® MetaMorph software (Meta Series Software 7.7.0; Molecular Devices) was used to quantify the data by taking densitometry readings of five separate locations with in the nucleus and cytoplasm of each cell.

SDS-PAGE and in-gel digestion

The eluted OGT sample was loaded onto a 4 - 12% Bis-Tris NuPAGE gel (NOVEX, SanDiego, CA) for electrophoresis and stained with Coomassie Brilliant Blue (Sigma-Aldrich). The gel bands corresponding to OGT were excised and subjected to in-gel tryptic digestion following a general protocol (MA & Hart 2014; Shevchenko et al., 2006). Briefly, OGT bands were destained with 50% (v/v) acetonitrile (ACN) prepared in 25 mM ammonium bicarbonate and 100 mM ammonium bicarbonate

for 15 min. Proteins were reduced with 20 mM DTT at 60°C for 1 h and then alkylated with 55 mM iodoacetamide at room temperature for 45 min in the dark. After dehydration, the proteins were digested with 12.5 ng/μl analytical grade porcine trypsin (Thermo Scientific Pierce, Rockford, IL) prepared in 50 mM ammonium bicarbonate overnight at 37°C. Peptides were then extracted from the gel pieces with 50%(v/v) ACN prepared in 5% formicacid, driedundera Centrivap concentrator (Labconco, Kansas City, MO) and stored at -20°C until use.

Mass spectrometry

The peptide samples extracted by in-gel digestion were suspended in 40 μl of solvent A (0.1% formic acid prepared in water, Optima LC/MS grade, Fisher Scientific, Pittsburgh, PA). Thereafter, 2 μl of the sample was loaded onto a house-packed 75 μm (inner diameter of microcapillary) × 15 cm C18 (5 μm, 100 Å) column and separated with a 5 - 30% gradient of solvent B (0.1% formic acid prepared in ACN) for 90 min at a flow rate of 300 nL/min. Mass spectra were recorded on an Orbitrap Fusion Tribrid mass spectrometer (Thermo Fisher Scientific, SanJose, CA) interfaced with a nano acquity UPLC (Waters, Milford, MA). The Orbitrap Fusion Tribrid mass spectrometer was operated in several modes all in Orbitrap, namely, full scan MS1, data-dependent acquisition high-energy collision dissociation scan, product ion-triggered MS3 ETD scan and product ion-triggered MS3 EThcD scan. The raw data were processed using the Trans-Proteomic Pipeline (v4.8.0 PHILAE) and compared with a database composed of human OGT1 (O15294-3, UniProt ID), about 500 decoy proteins and common contaminants. Carbamidomethyl of cysteine was considered the fixed modification, and variable modification was set for oxidation of methionine and *O*-GlcNAcylation of serine and threonine.

Statistical analysis

Each experiment was repeated three to four times with consistent results. Data are representative of the mean values obtained. Differences between groups were evaluated using the two-tailed unpaired Student's *t*-test. *P* values <0.05 were considered to indicate statistical significance for all statistical evaluations. (*$P<0.01$ and **$P<0.05$)

Results

4.1. The DFP motif plays a role in the nuclear localization of OGT

To identify the NLS of OGT, we generated deletion mutants of OGT and determined their subcellular localization. HeLa cells were transfected with OGT fused to GFP at the N-terminus and subjected to subcellular fractionation. The first deletion mutant (residues 1 - 453) contained 13 TPRs, including the sixth and seventh repeats (the local dyad axis of the homodimer), and localized in the nucleus and cytoplasm. The second deletion mutant lacked the N-terminal 453 aminoacids (residues 454 - 1036) and localized exclusively in the cytoplasm. The third construct contained three more amino acids downstream of the thirteenth TPR (residues 451 - 1036) and was detected in the nucleus and cytoplasm (Figure 1). Taken together, these data suggest that the residues 451 - 453 are important for the nuclear import of OGT. To further demonstrate that these three amino acids are the NLS of OGT, we generated Mono-OGT, which excluded the possibility of an interaction between mutant OGT and endogenous OGT, because the tendency of homodimerization of OGT is decreased when two hydrophobic residues are replaced with negatively charged residues (W198E and I201D) (Jinek et al., 2004). The interaction between Mono-OGT and endogenous OGT was significantly decreased compared to WT-OGT (Figure 3). Furthermore, the three amino acids of interest (Asp451, Phe452 and Pro453) were mutated to alanine (451-453AAA) or deleted (Δ451-453; Figure 2A). Both Mono-OGT 451-453AAA and Mono-OGT Δ451-453 were distributed largely in the cytoplasm (Figure 2B - E). Taken together, these results indicate that we identified the NLS of OGT that plays a role in localizing OGT to the nucleus.

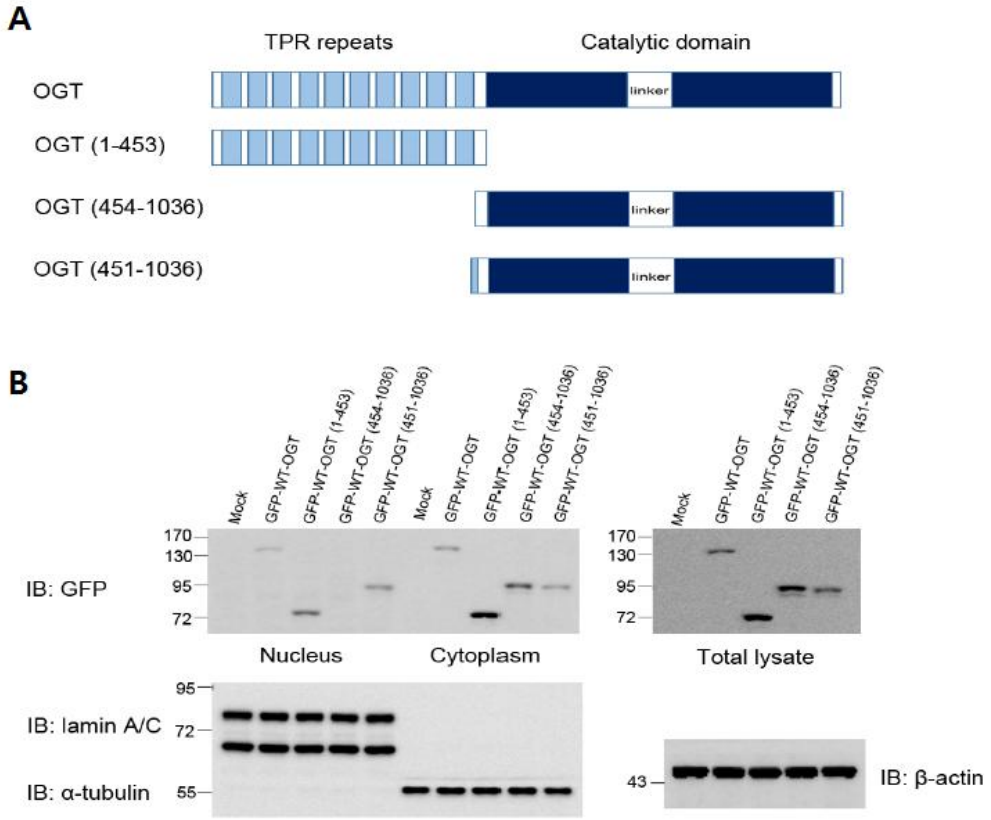

Figure 1. Subcellular localization of OGT deletoin mutants

(A) Schematic representation of OGT constructs used. The first deletion mutant (residue 1-453) only contained 13 TPR repeats. The second and third constructs lacked the N-terminal TPR repeats and contained catalytic domain. The third construct contained three more amino acids downstream of the thirteenth TPR (residues 451-1035).

(B) GFP-tagged WT-OGT and various OGT deletion mutants were expressed in HeLa cells. Cells were subjected to subcellular fractionation. Western blotting of aliquots of the fractions was performed with an α-Flag antibody to detect OGT and with α-lamin

A/C, α-α-tubulin and α-β-actin as markers of the nuclear, cytoplasmic and total fractions, respectively.

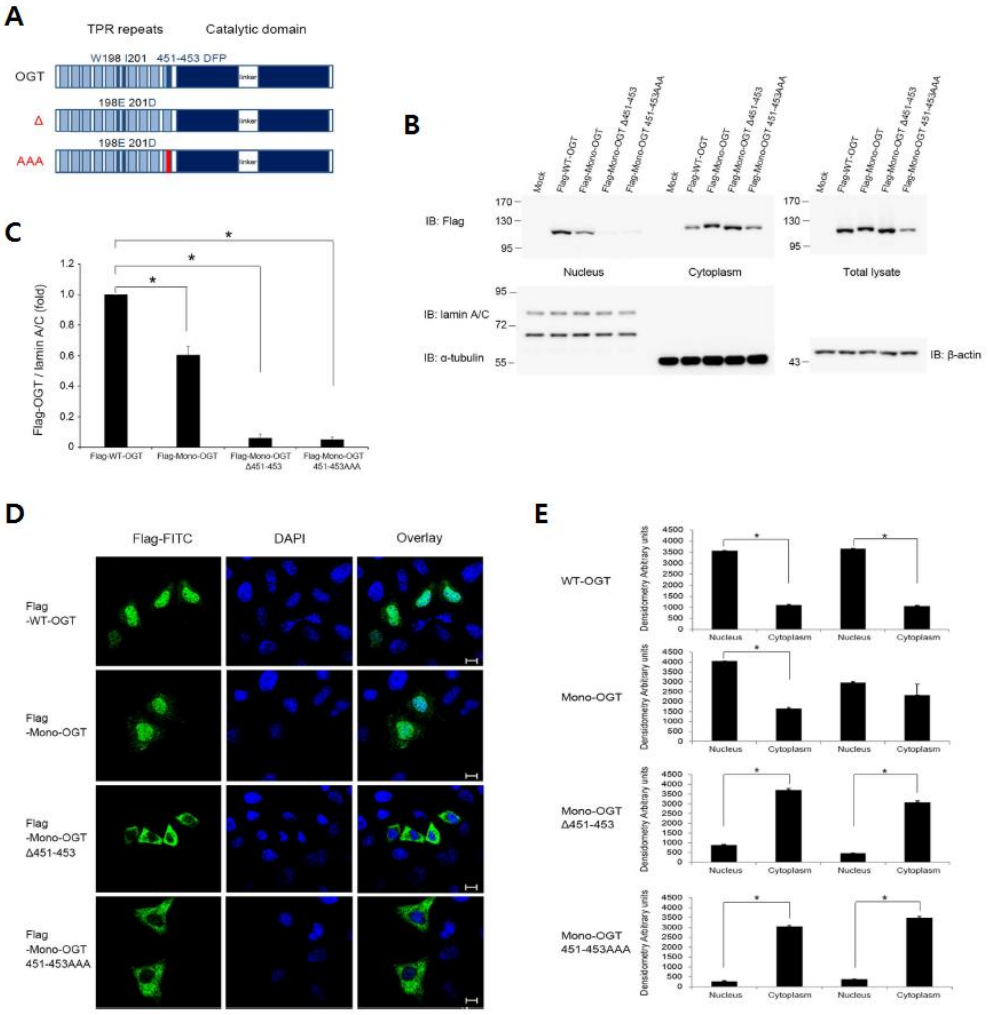

Figure 2. Identification of the NLS of OGT

(A) Schematic representation of the OGT constructs used. In Mono-OGT, Trp198 and Ile201 were mutated to glutamate and aspartate, respectively. Δ, deleted DFP motif; AAA, substituted DFP motif.

(B) WT-OGT and various OGT mutants were expressed as Flag-tagged proteins in HeLa cells grown in 10 cm plates. Subcellular

fractionation was performed and aliquots of the fractions were analysed by western blotting with an α-Flag antibody to detect OGT, and with α-lamin A/C, α-α-tubulin and α-β-actin antibodies as markers of the nuclear, cytoplasmic and total fractions, respectively. Images of western blot immunoblotted with an α-Flag antibody, was stripped, and then re-immunoblotted with α-lamin A/C, α-α-tubulin and α-β-actin antibodies respectively.

(C) The band intensities of nuclear imported Flag-OGT in (b) were quantified by densitometry and normalized to the laminA/C band intensity. $*P<0.01$ (Student's t-test), mean ± s.d.

(D) HeLa cells were grown on coverslips and transfected with Flag-tagged WT-OGT, Mono-OGT, Mono-OGT Δ451-453 or Mono-OGT 451-453 AAA. Cells were stained with an α-Flag antibody (green) and then analysed by fluorescence microscopy. Nuclei were stained with DAPI (blue). Scale bar, 10 μm.

(E) Densitometry readings of five separate locations within the nucleus were averaged and this was compared with the mean measurement in five separate locations within the cytoplasm of each cell. Data were quantified using MetaMorph software. Data show mean ± s.d.; n=5 locations in the cell. $*P<0.01$ (Student's t-test).

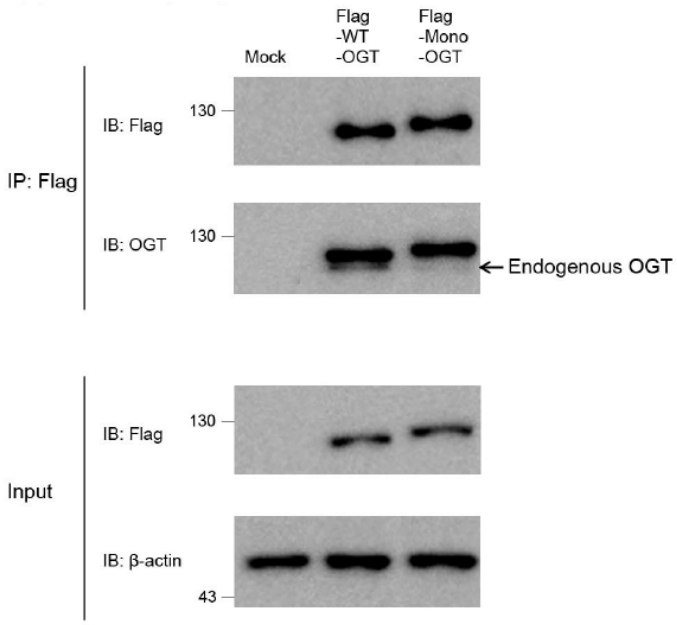

Figure 3. Overexpressed OGT interacts with endogenous OGT

Flag-tagged WT-OGT or Mono-OGT (Trp198 and Ile201 mutated to glutamate and aspartate, respectively) was overexpressed in HeLa cells and immunoprecipitated with an α-Flag antibody. Levels of precipitated OGT were determined by an α-Flag antibody, and interacting endogenous OGT was detected by an α-OGT antibody.

4.2. The DFP motif can function as a NLS independently

To validate the importance of the DFP motif of OGT and to examine whether it can act as a NLS independently, we used Flag-tagged β-galactosidase. This protein was too big to freely diffuse into the nucleus and localised exclusively in the cytoplasm when expressed in HeLa cells. However, the addition of DFP to the N-terminus of Flag-tagged β-galactosidase induced its nuclear translocation (Figure 4A - C), and this was prevented by mutation of DFP to AFP, DAP, DFA or AAA (Figure 5). Then we wanted to test whether the putative NLS of OGT reported in 1997 (Lubas et al,. 1997) has an actual function as nuclear import. However, fusion of putative NLS (residues 477-493) to the Flag-tagged β-galactosidase did not cause import into the nucleus (Figure 5B). We also used Flag tagged double-stranded RNA-specific editase 1 (ADARB1) to test the function of DFP motif in ADARB1. ADARB1 mutated DFP (residues 171 - 173) to AAA showed greatly reduced nuclear import than WT-ADARB1 (Figure 12). ADARB1 was still localized in the nucleus because ADARB1 interacts with other endogenous ADARB1 in the cells. These results clearly demonstrate that the DFP motif functions as nuclear import independently.

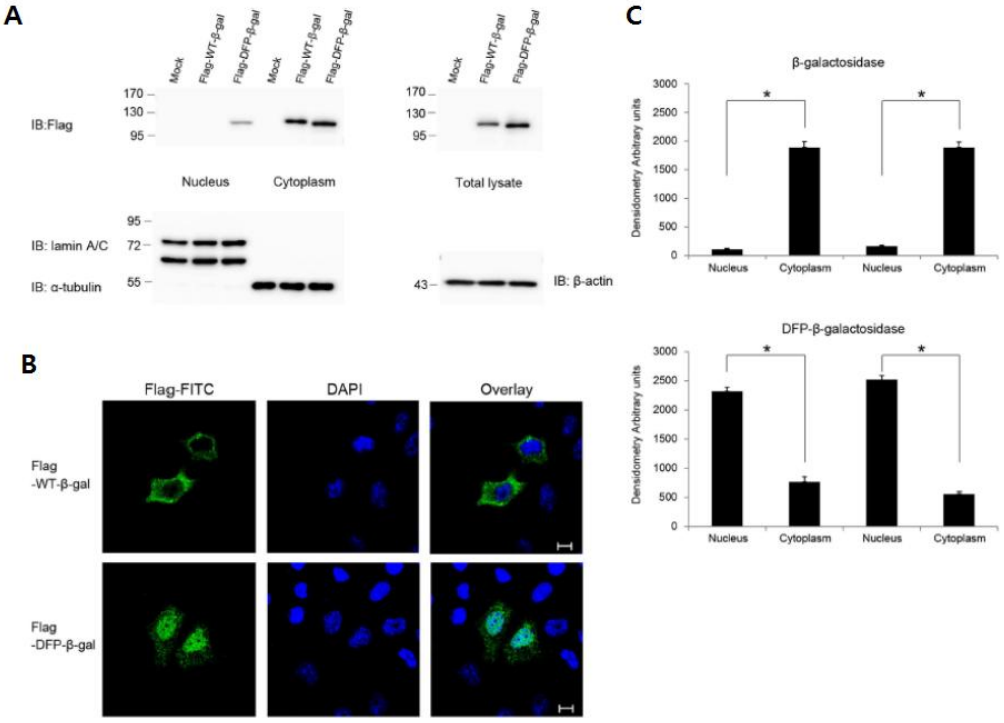

Figure 4. The DFP motif is an independent NLS

(A) Subcellular fractionation was performed of HeLa cells transfected with Flag-tagged WT-β-galactosidase or DFP-fused β-galactosidase. Western blotting of aliquots of the fractions was performed with an α-Flag antibody to detect the β-galactosidase proteins, and with α-lamin A/C, α-α-tubulin and α-β-actin antibodies as markers of the nuclear, cytoplasmic and total fractions, respectively. Images of western blot immunoblotted with an α-Flag antibody, was stripped, and then re-immunoblotted with α-lamin A/C, α-α-tubulin and α-β-actin antibodies respectively.

(B) Immunofluorescence confirmed the subcellular fractionation results. HeLa cells transiently overexpressing Flag-tagged β-galactosidase constructs were fixed and stained with both an α-Flag antibody (green)

and DAPI (blue). Scale bar, 10 μm.

(C) The mean of densitometry readings in five separate locations within the nucleus was obtained and this was compared with the mean measurement of five separate locations within the cytoplasm of each cell. Data were quantified using MetaMorph software. Data show mean ± s.d.; n=5 locations in the cell. $*P<0.01$ (Student's t-test).

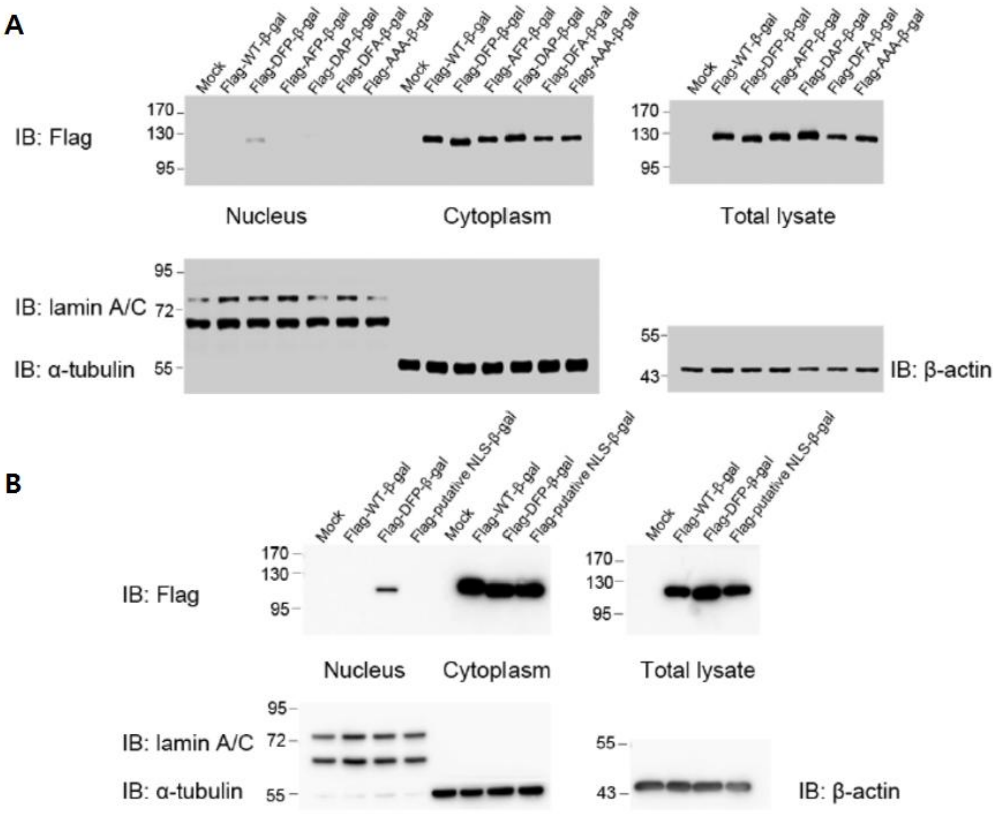

Figure 5. The DFP motif can induce β-galactosidase's nuclear import

(A) Subcellular fractionation was performed of HeLa cells transfected with Flag-tagged WT-β-galactosidase, DFP-β-galactosidase, AFP-β-galactosidase, DAP-β-galactosidase, DFA-β-galactosidase or AAA-β-galactosidase. Western blotting of aliquots of the fractions was performed with an α-Flag antibody to detect the -β-galactosidase proteins, and with α-lamin A/C, α-α-tubulin and α-β-actin antibodies as markers of the nuclear, cytoplasmic and total fractions, respectively

(B) HeLa cells were transfected with Flag-tagged WT-β-galactosidase,

DFP-β-galactosidase, or putative NLS-β-galactosidase and then subjected to subcellular fractionation as described in (A). DFP; 451-453 residues and putative NLS; 477-493 residues.

4.3. Importin α5 interacts with OGT

Because nuclear transport of proteins commonly requires their interaction with importin αs(Christophe et al,. 2000; Goldfarb et al., 2004), we determined whether OGT associates with importin αs. The classical nucleocytoplasmic import pathway is mediated by the importin α/β heterodimer (Cautain et al., 2015; Gorlich et al., 1995). While only one importin β isoform exists, six human importin αs have been reported(Quensel et al., 2004). Although the importin αs differ in terms of their cell-andtissue-specific expression patterns, most are expressed ubiquitously, except for importin α6, which is only present in testes (Kohler et al., 1997). Therefore, we tested the association of OGT with the other five importin αs. No binding was observed between OGT and importin β, α1, α3, α4, or α7 (Figure 6A, B). However, overexpressed OGT interacted with overexpressed or endogenous importin α5 (Figure 6A-D).To determine whether importin α5 is also required for the nuclear localization of OGT, we depleted importin α5 in HeLa cells by RNA interference (RNAi). In cells treated with small interfering RNA (siRNA) targeting importin α5, the amounts of overexpressed OGT localized in the nucleus and cytosol were decreased and increased, respectively (Figure 6E - G). Thus, our results suggest that importin α5 is an important karyopherin of OGT.

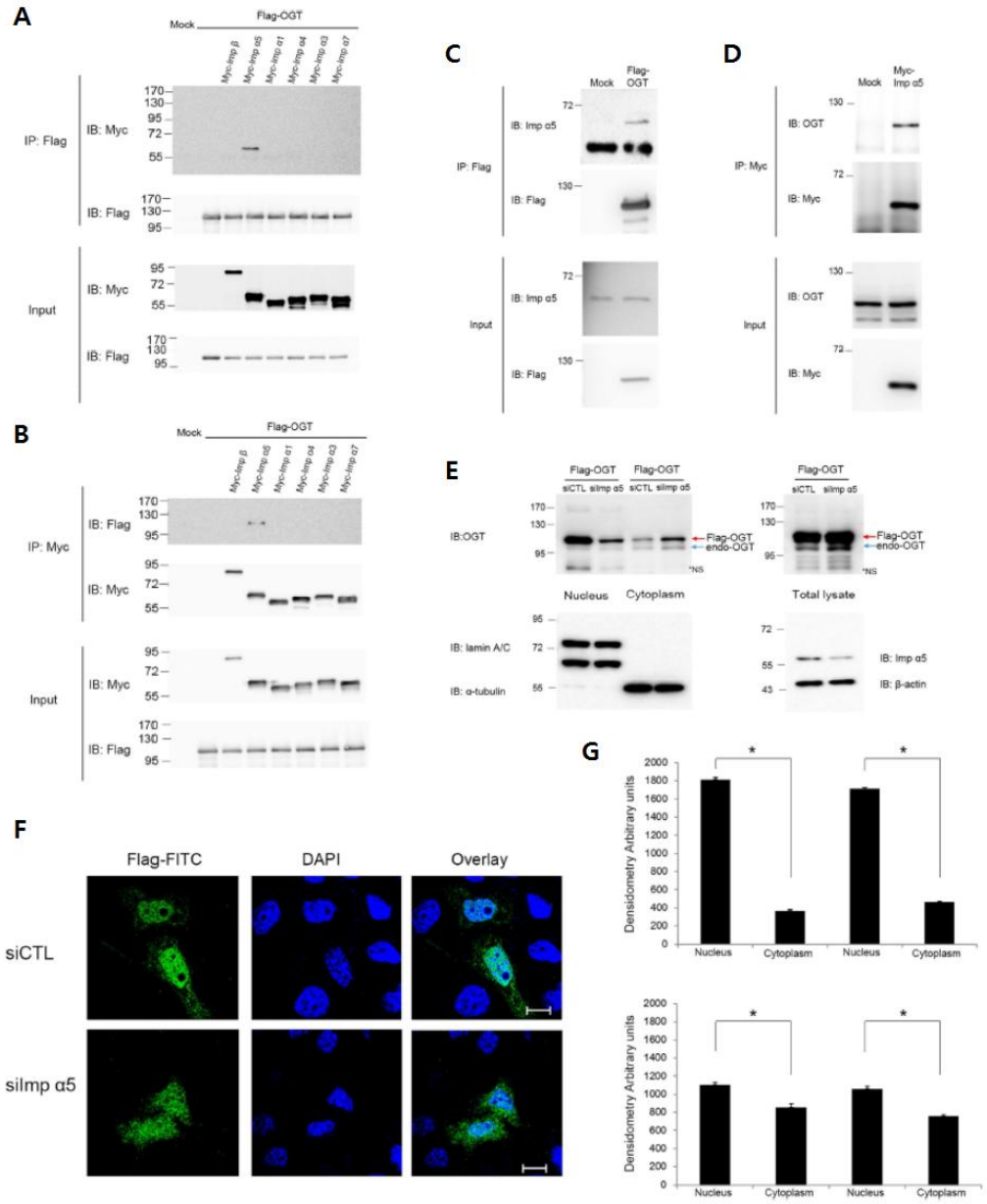

Figure 6. Binding of importin proteins to OGT

(A) HeLa cells were co-transfected with Flag-tagged OGT and

Myc-tagged importin α or β. Cell lysates were immunoprecipitated with an α-Flag antibody. Co-immunoprecipitated importin α or β, as well as the loading amounts, were analysed by western blotting with an α-Myc antibody. An α-Flag antibody immunoblotting confirmed that equal amounts of OGT constructs were immunoprecipitated.

(B) Cells were transfected as in (A) were immunoprecipitated with an α-Myc antibody. Co-immunoprecipitated OGT was blotted with an α-Flag antibody. An α-Myc antibody immunoblotting confirmed that equal amounts of importin α and β were immunoprecipitated.

(C) HeLa cells were transfected with Flag-tagged OGT and immunoprecipitated with an α-Flag antibody. Bound endogenous importin α5 was detected by an α-importin α5 antibody. Total lysates were blotted with an α-importin α5 antibody as a loading control.

(D) HeLa cells transiently overexpressing Myc-tagged importin α5 were immunoprecipitated with an α-Myc antibody. Co-immunoprecipitated endogenous OGT was detected by an α-OGT antibody. Total lysates were blotted with an α-OGT antibody to monitor the amount of OGT.

(E) HeLa cells were transfected twice with siRNA targeting importin α5 or control siRNA. After 3 days, cells were transfected with Flag-tagged OGT. After another day, cells were subjected to subcellular fractionation. Western blotting was performed on the cytoplasmic and nuclear fractions. Total lysates were blotted with an α-importin α5 antibody to monitor the reduction in endogenous importin α5 and with an α-β-actin antibody as a loading control. *NS; non-specific.

(F) Immunofluorescence confirmed the subcellular fractionation results. Cells were prepared as described in (E), fixed, stained with an α-Flag antibody (green) and DAPI (blue). Scale bar, 10 μm.

(G) The mean of densitometry readings in five separate locations within the nucleus was obtained and was compared with the mean readings of five separate locations within the cytoplasm of each cell. Data were quantified using MetaMorph software. Data show mean ± s.d.; n=5 locations in the cell. $*P<0.01$ (Student's t-test).

4.4. The DFP motif is required for the interaction of OGT with importin α5

The finding that importin α5 is involved in the nuclear import of OGT prompted us to examine whether the binding of importin α5 is dependent on the DFP motif of OGT. We first examined the interaction of the various OGT mutants with importin α5. Co-immunoprecipitation experiments revealed that WT-OGT interacted more strongly with importin α5 than Mono-OGT and that Mono-OGT in which the NLS was mutated or deleted showed significantly reduced association with importin α5 (Figure 7A, B). A slight interaction exists between Mono-OGT Δ451-453, Mono-OGT 451-453 AAA and importin α5 because Mono-OGT still can interact with endogenous OGT (Figure 3). These results were confirmed by in vitro binding assays (Figure 7C). Pull-down experiments were performed in which glutathione S-transferase (GST)-importin α5 fusion protein was incubated with the lysates of HeLa cells transiently overexpressing WT-OGT, Mono-OGT, Mono-OGT Δ451-453 or Mono-OGT 451-453 AAA. No interaction was observed between GST-importin α5 and Mono-OGT Δ451-453 or Mono-OGT 451-453 AAA, as expected. In all experiments, importin α5 interacted more weakly with Mono-OGT than with WT-OGT. This reduced binding affinity of Mono-OGT for importin α5 would explain why the nuclear localization of Mono-OGT was less extensive than that of WT-OGT (Figure 2B, C). Taken together, these results indicate that importin α5 has a functional interaction with the NLS of OGT, which affects the nuclear localization of monomeric OGT.

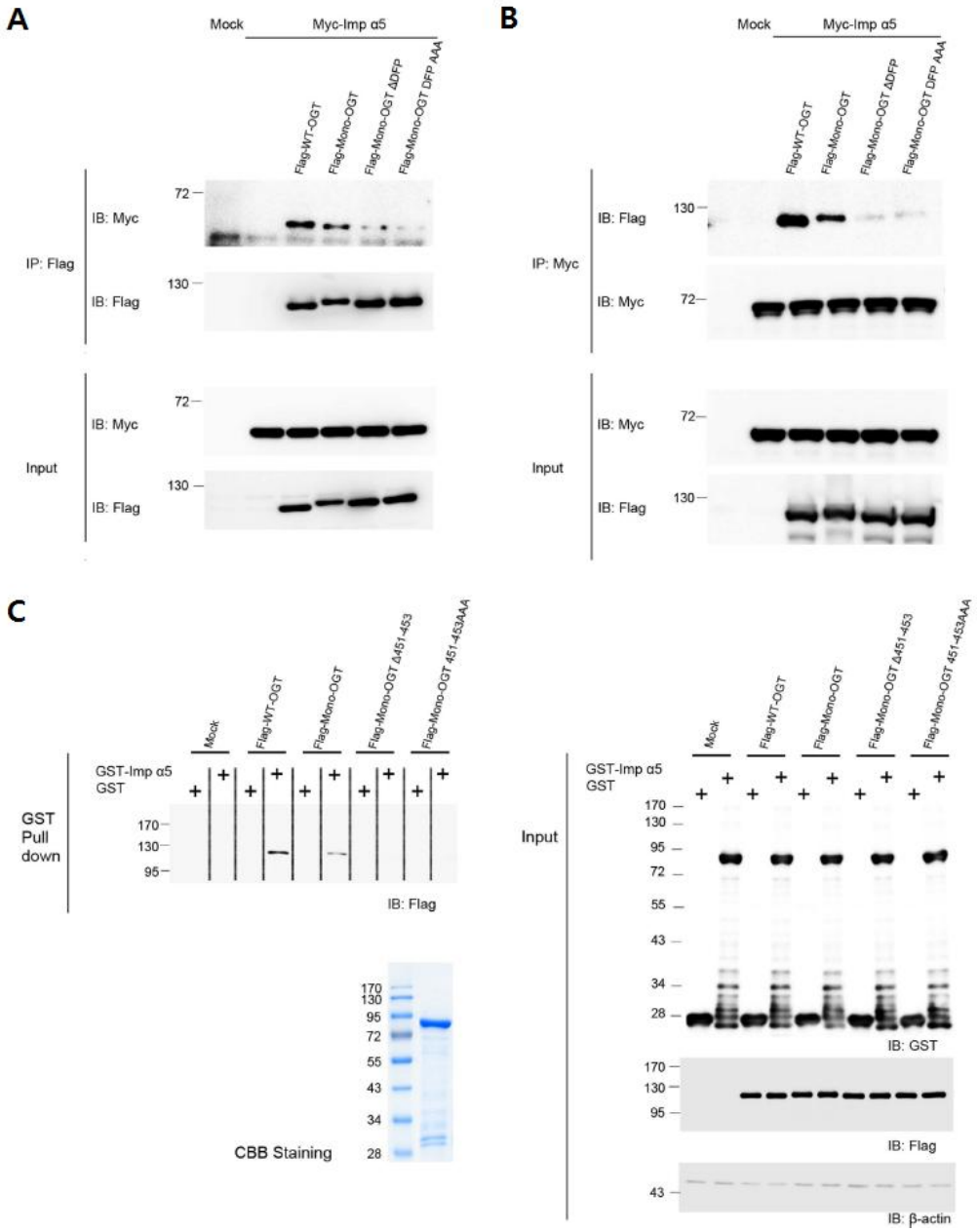

Figure 7. The DFP motif of OGT interacts with importin α5

(A) HeLa cells transiently overexpressing Flag-tagged WT-OGT,

Mono-OGT, Mono-OGT Δ451-453 or Mono-OGT 451-453 AAA together with Myc-tagged importin α5 were immunoprecipitated with an α-Myc antibody and the beads were stringently washed three times. Co-immunoprecipitated OGT constructs were detected by an α-Flag antibody. Blotting with an α-Myc antibody revealed that equal amounts of importin α5 were immunoprecipitated.

(B) HeLa cells transfected with Flag-tagged WT-OGT, Mono-OGT, Mono-OGT Δ451-453 or Mono-OGT 451-453 AAA together with Myc-tagged importin α5 were immunoprecipitated with an α-Flag antibody. Following stringent washes, co-immunoprecipitated importin α 5 was detected by an α-Myc antibody. Blotting with an α-Flag antibody revealed that equal amounts of the OGT constructs were immunoprecipitated.

(C) HeLa cells were transfected with Flag-tagged WT-OGT, Mono-OGT, Mono-OGT Δ451-453 or Mono-OGT 451-453 AAA. Cell lysates were incubated with immobilized recombinant GST-importin α5. GST-importin α5 was precipitated, and the associated OGT constructs were detected by western blotting using an α-Flag antibody. GST-importin α5 was detected by Coomassie staining to verify the amount of protein used in the assay.

4.5. *O*-GlcNAclation of OGT occurs at Ser389

OGT is reportedly modified by *O*-GlcNAc (Khidekel et al., 2007; Tai et al., 2004). However, the sites and functions of *O*-GlcNAc modification of OGT has not been elucidated. To identify the *O*-GlcNAcylated site(s) of OGT, we used HEK293 cells instead of HeLa cells to acquire the necessary amount of Flag-tagged OGT. We separated Flag-tagged OGT immunoprecipitated from HEK293 cell lysates by SDS-PAGE and analysed the protein by mass spectrometry in electron-transfer dissociation (ETD) fragmentation mode. We identified an *O*-GlcNAcylated peptide (amino acids 380 - 396) of OGT (ISPTFADAY<u>S</u>NMGNTLK; Xcorr, 2.808; DeltaCn, 0.477), where the Ser389 residue was modified with *O*-GlcNAc assigned c+ and z+ product ions including distinct *O*-GlcNAc oxonium ions[2](m/z 204.09, 186.08, 168.06, 138.05 and 126.05) (Figure 8A). Next, we created site-specific point mutants of OGT. Mutation of Ser381 and Ser389 with alanine and Thr383, and Thr394 with valine, resulted in a reduction in *O*-GlcNAc modification (Figure 8B, C). From this investigation, we determined that Ser389 is the major *O*-GlcNAc modification site of OGT. However, we cannot rule out the possibility that other *O*-GlcNAcylation sites exist because OGT was still modified with *O*-GlcNAc, despite mutation of this site.

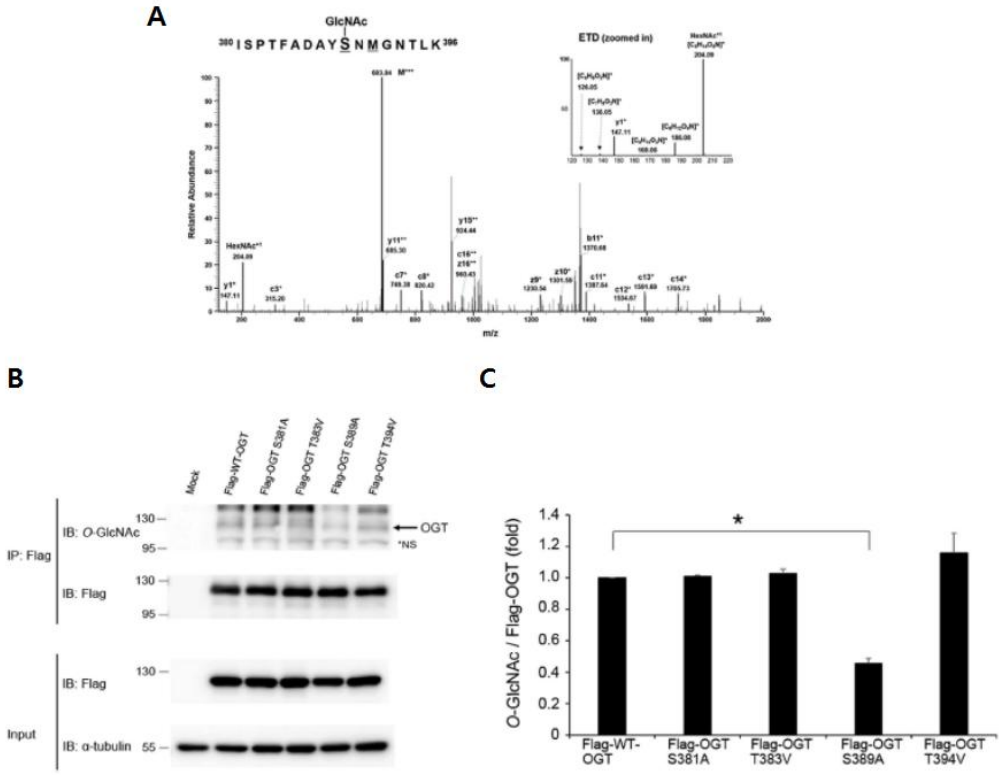

Figure 8. OGT undergoes *O*-GlcNAc modification

(A) The ETD MS/MS spectrum of an *O*-GlcNAcylated peptide of OGT1 (residues 380 - 396) with the triply charged precursor ion m/z 638.9881(M+3H)$^{3+}$isshown.The c- and z-type product ions were assigned. The *O*-GlcNAc oxonium ion (m/z, 204.09) and a series of its fragments (m/z, 186.08, 168.06, 138.05 and 126.05) were also assigned.

(B) Flag-tagged WT-OGT or OGT point mutants were overexpressed in HEK293 cells. WT-OGT and OGT point mutants were immunoprecipitated with an α-Flag antibody and blotted with an α -*O*-GlcNAc antibody. Blotting with an α-Flag antibody confirmed that

equal amounts of the OGT constructs were immunoprecipitated. *NS; non-specific.

(C) The band intensities *O*-GlcNAc in (B) were quantified by densitometry and normalized to immunoprecipitated Flag band intensity. *P<0.01 (Student's t-test), mean ± s.d.

4.6. *O*-GlcNAc modification of the TPR domain of OGT is important for its nuclear localization

Next, we examined to what extent *O*-GlcNAc modification of OGT contributes to its nuclear localization. Because Mono-OGT showed less nuclear import than WT-OGT (Figure 2B-E) and has lower *O*-GlcNAc modification level than that of WT-OGT (Figure 9). Combined with the previous results, we assumed that *O*-GlcNAcylation of OGT may impact its nuclear localization. To address this issue, we constructed the Mono-OGT S389A mutant. To increase *O*-GlcNAc modification of OGT, cells were treated with Thamet-G, a selective inhibitor of *O*-GlcNAcase. Then nuclear localization of both WT-OGT and Mono-OGT was increased in Thiamet-G-treated cells (Figure 10A, B). However, the nuclear localization of Mono-OGT S389A was almost abolished in both Thiamet-G-treated and untreated cells (Figure 10A). To decrease *O*-GlcNAc modification of OGT, cells were treated with 5-thio-GlcNAc (Gloster et al., 2011), an inhibitor of OGT. The nuclear localization of both WT-OGT and Mono-OGT was decreased in 5-thio-GlcNAc-treatedcells, and the nuclear localization of Mono-OGT S389A was completely prevented (Figure 10C, D). These findings were further supported by fluorescence microscopy analysis (Figure 10 E, F). We predicted that the nuclear localization of OGT was decreased by a change in its conformation upon exposure of the NLS (residues 451 - 453). OGT S389A had the same enzyme activity as WT-OGT (Figure 11) and the substitution of Alanine for Ser389 in OGT does not affect protein-protein interaction with other proteins (Figure 11C). This indicated that the decrease of the nuclear localization of OGT was not due to distortion of its structure, but due to exposure of its NLS. Collectively, our data indicate that the nuclear localization of OGT is mainly regulated by *O*-GlcNAc modification of Ser389. Our results are summarised in Figure 13. *O*-GlcNAc modification at Ser389 probably

results in exposure of the hidden NLS of OGT and its association with importin α5 and β, resulting in its nuclear localization.

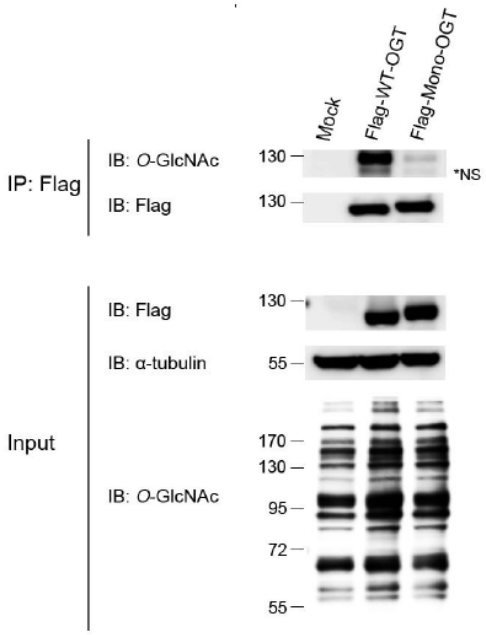

Figure 9. Decreased *O*-GlcNAcylation of Mono-OGT

Flag-tagged WT-OGT or Mono-OGT was overexpressed in HeLa cells and immunoprecipitated with an α-Flag antibody. Immunoprecipitates were blotted with an α-*O*-GlcNAc antibody. Blotting with an α-Flag antibody confirmed that equal amounts of OGT were precipitated. *NS; non-specific.

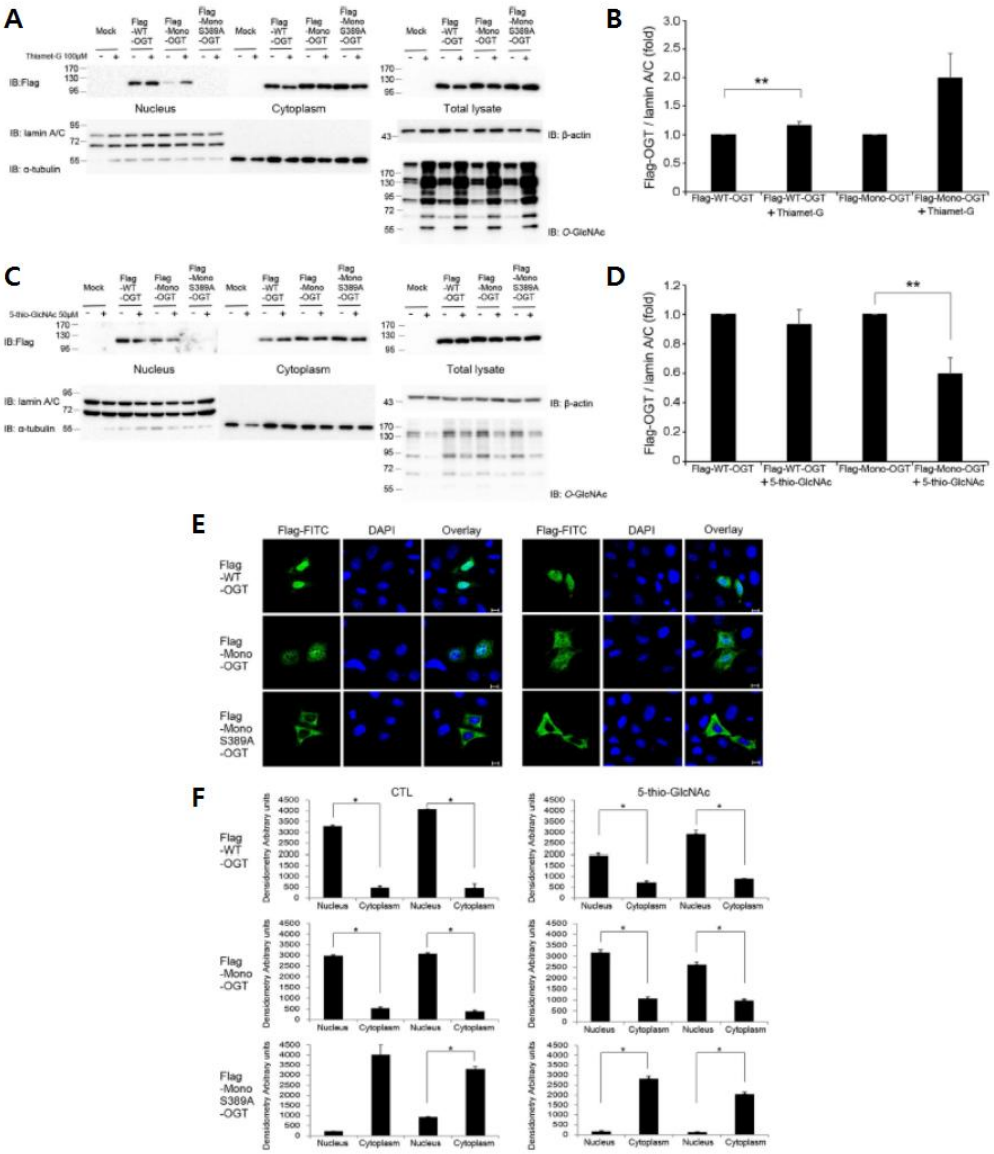

Figure 10. *O*-GlcNAcylation of Ser389 affects the nuclear localization of OGT

(A) HeLa cells were treated with Thiamet-G (100 μM, 4 h) and were then transfected with Flag-tagged WT-OGT, Mono-OGT or

Mono-OGT S389A for 24 hours. Cell extracts were subjected to subcellular fractionation. Western blotting of aliquots of the fractions was performed with an α-Flag antibody to detect the OGT constructs, and with α-α-tubulin and α-lamin A/C antibodies as cytoplasmic and nuclear markers, respectively. Images of western blot immunoblotted with an α-Flag antibody, was stripped, and then re-immunoblotted with α-lamin A/C, α-α-tubulin and α-β-actin antibodies respectively.

(B) The band intensities of nuclear imported Flag-OGT in (A) were quantified by densitometry and normalised to the laminA/C band intensity. $**P<0.05$ (Student's t-test), mean ± s.d.

(C) HeLa cells were treated with 5-thio-GlcNAc (50 μM, 4h) and were then transfected with Flag-tagged WT-OGT, Mono-OGT or Mono-OGT S389A for 24 hours. Cell extracts were subjected to subcellular fractionation as described in (A).

(D) The band intensities of nuclear imported Flag-OGT in (C) were quantified by densitometry and normalized to the laminA/C band intensity. $**P<0.05$ (Student's t-test), mean ± s.d.

(E) Immunofluorescence analysis confirmed the subcellular fractionation results shown in (B). HeLa cells were treated with 5-thio-GlcNAc (50 μM, 4h) or untreated, and then transfected with Flag-tagged WT-OGT, Mono-OGT or Mono-OGT S389A. Thereafter, cells were fixed, stained with an α-Flag antibody (green) and DAPI (blue), and visualized. Scale bar, 10 μm.

(F) The mean of densitometry readings in five separate locations within the nucleus was obtained and this was compared with the mean measurement of five separate locations within the cytoplasm of each cell. Data were quantified using MetaMorph software. Data show mean ± s.d.; n=5 locations in the cell. $*P<0.01$ (Student's t-test)

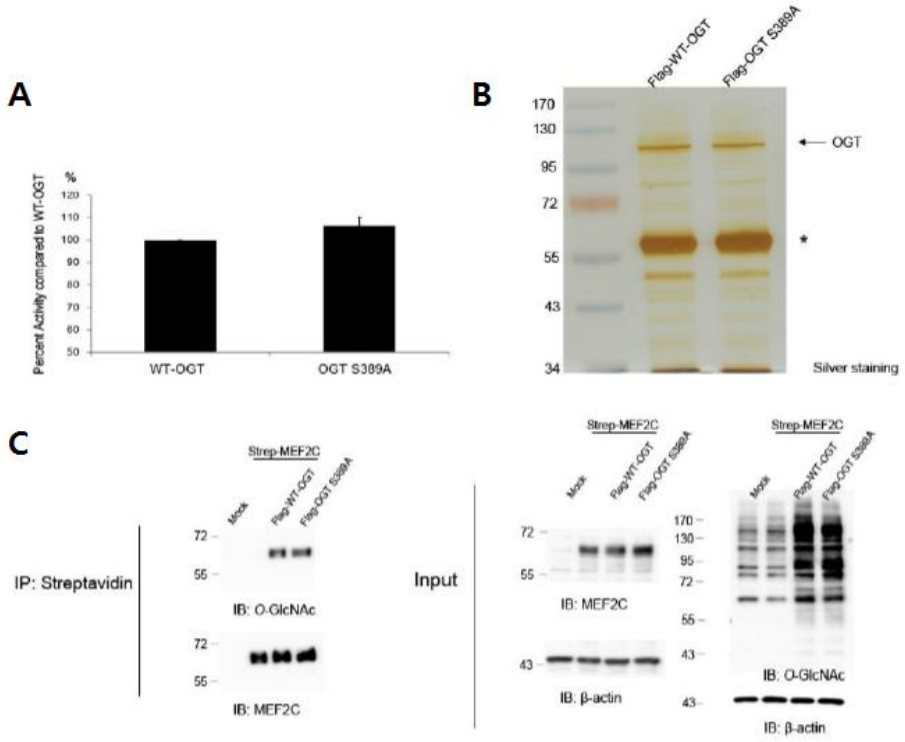

Figure 11. The substitution Alanine for Ser389 in OGT dose not affect the enzyme acitivity and protein-protein interaction

(A) Flag-tagged WT-OGT or OGT S389A was expressed in HeLa cells. OGT activity was measured using the casein kinase 2 peptide as a substrate. The y-axis represents activity relative to that of WT-OGT. Data show mean ± s.d.; n=3, data pooled across three independent experiments.

(B) Flag-tagged WT-OGT or OGT S389A were co-expressed with Strep-tagged MEF2C in HeLa cells. Strep-tagged MEF2C was then immunoprecipitated with streptavidin agarose and immunoblotted with for α-*O*-GlcNAc antibody. Blotting with an α-MEF2C antibody confirmed that equal amount of the MEF2C constructs were

immunoprecipitated.

(C) HeLa cells were transfected with Flag-tagged WT-OGT or OGT S389A. Cell lysates were immunoprecipitated with an α-Flag antibody and the beads were mildly washed three times. Co-immunoprecipitated proteins were separated by SDS-PAGE and were then stained with silver nitrate. *; IgG heavy chain

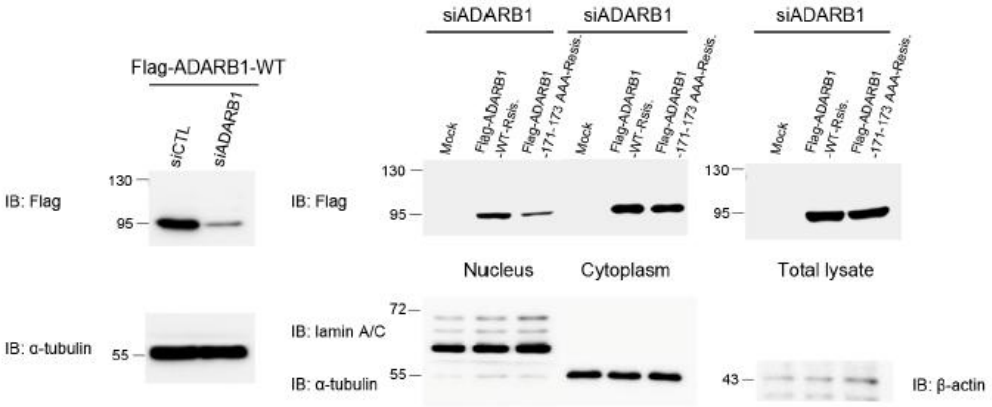

Figure 12. The DFP motif mediates the nuclear import of ADARB1

HEK293 cells were transfected with control siRNA or siRNA targeting ADARB1 using Lipofectamine. Forty-eight hours later, cells were transfected with the siRNA-resistant construct of Flag-tagged ADARB1, or ADARB1-171-173 AAA respectively. Subsequently, cells were subjected to subcellular fractionation. Western blotting of aliquots of the fractions was performed with an α-Flag antibody to detect ADARB1 and with α-α-tubulin, α-lamin A/C and α-β-actin antibodies as cytoplasmic, nuclear and total markers, respectively.

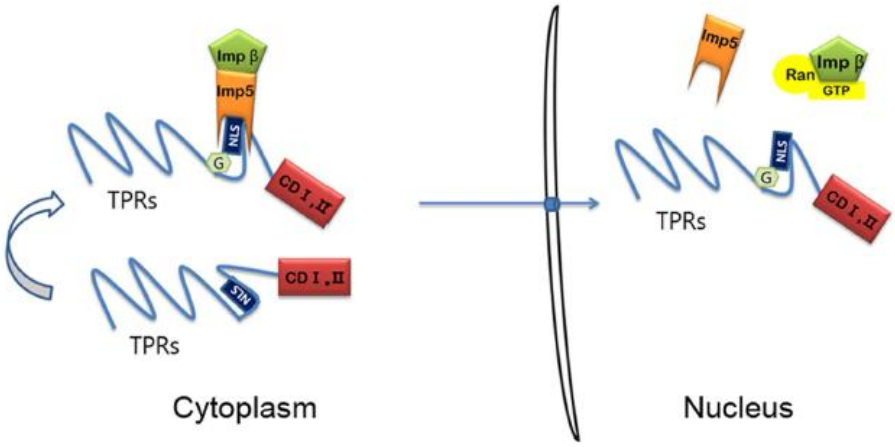

Figure 13. Working model for the nuclear localization of OGT

In the cytosol, OGT can be *O*-GlcNAcylated on Ser389, which is located in the vicinity of the DFP motif. Without *O*-GlcNAc modification, binding of importin α5 may be hindered because the DFP motif of OGT is hidden. However, once *O*-GlcNAc modification occurs, OGT can interact with importin α5 and hence localise in the nucleus. CD Ⅰ, Ⅱ; catalytic domain Ⅰ, Ⅱ.

5. Discussion

OGT transfers GlcNAc from uridine diphosphate-N-acetyl glucosamine to the hydroxyl group of a serine or threonine residue on cytoplasmic and nucleus protein substrates (Haltiwanger et al., 1992; Kreppel et al., 1997). The TPR domain of the enzyme crystallizes as adimer with an interface between the two subunits (Jinek el al., 2004). The catalytic domain has a nucleotide-binding domain and there are hinge regions between the twelfth and thirteenth TPRs, where OGT pivotsdramatically (Lazarus et al., 2011). Based on these previous studies, we investigated the molecular changes that allow the nuclear import of OGT, which is not fully understood. We identified the NLS of OGT (DFP at position 451 - 453). Deletion or alanine substitution of DFP abolished the nuclear localization of OGT and β-galactosidase localized in the nucleus when fused to DFP, suggesting that this NLS plays an essential role in nuclear import. We used Mono-OGT (W198EandI201D) (Jinek el al., 2004) because endogenous OGT can interact with the exogenously expressed proteins and transport them to the nucleus. Immunoprecipitated Flag-tagged Mono-OGT showed a very weak binding affinity for endogenous OGT (Figure 3), confirming the weak interaction between Mono-OGT and endogenous OGT. This is why very faint bands of Mono-OGT 451-453 AAA and Mono-OGT Δ 451-453 were detected in the nuclearfraction (Figure 2B). Moreover, because Mono-OGT weakly interacted with endogenous OGT, we predicted that the extent of *O*-GlcNAc modification of Mono-OGT is much lower than that of WT-OGT. To test this possibility, we immunoprecipitated Flag from lysates of cells transiently overexpressing Flag-tagged WT-OGT and Mono-OGT. The level of *O*-GlcNAcylated Mono-OGT was considerably lower than that of *O*-GlcNAcylated WT-OGT (Figure 9). This reduced *O*-GlcNAc modification of Mono-OGT decreased its interaction with importin α5 (Figure 7A-C).

Together, these experiments explain why the nuclear importation rate of Mono-OGT was lower than that of WT-OGT. On the other hand, the nuclear localization of transfected Mono-OGT Δ451-453 and Mono-OGT 451-453 AAA was significantly impaired compared with that of WT-OGT and Mono-OGT (Figure 2B - E). The identified DFP motif of OGT is not a classical NLS and many proteins that have the same motif localize in the nucleus or remain in the cytoplasm. Surprisingly, the nuclear import of exogenously expressed double-stranded RNA-specific editase 1 (ADARB1) was decreased when its DFP residues at positions 171 - 173 were mutated to AAA (Figure 12). In these experiments, endogenous ADARB1 was knocked down using RNAi because this protein reportedly forms a homodimer (Cho et al., 2003; Valente et al., 2007). Regulation of then uclear import of other proteins that have a DFP motif should be studied. We postulate that both the NLS and *O*-GlcNAcylation of Ser389 contribute to the nuclear localization of OGT. *O*-GlcNAc modification might induce a conformational change to facilitate nuclear translocation, similar to other nucleocytoplasmic proteins, such as phosphorylation of extracellular signal-regulated kinase 5 and human telomerase reverse transcriptase (Chung et al., 2012; Kondoh et al., 2006). Additionally, a recent publication showed that phosphorylation ofT hr444 of OGT is important for its nuclear localization (Bullen et al., 2014). We assume that Thr444 is in close proximity to the DFP motif at positions 451 - 453 and acts the same as Ser389. In summary, we identified a unique NLS that is responsible for the nuclear localization of OGT. This NLS controls the nuclear localization of overexpressed β-galactosidase containing the DFP motif. We also showed that OGT is imported into the nucleus using the DFP motif mediated by importin α5. Our data indicate that *O*-GlcNAcylation of the TPR domain of OGT (Ser389) is required for its nuclear localization. These findings establish a foundation for how nucleocytoplasmic proteins are regulated and exist in the nucleus and

cytosol simultaneously without any other sequestering proteins.

6. References

Adam, S.A., and Gerace, L. (1991). Cytosolic proteins that specifically bind nuclear location signals are receptors for nuclear import. Cell *66*, 837-847.

Boussif, O., Lezoualc'h, F., Zanta, M.A., Mergny, M.D., Scherman, D., Demeneix, B., and Behr, J.P. (1995). A versatile vector for gene and oligonucleotide transfer into cells in culture and in vivo: polyethylenimine. Proc Natl Acad Sci U S A *92*, 7297-7301.

Bullen, J.W., Balsbaugh, J.L., Chanda, D., Shabanowitz, J., Hunt, D.F., Neumann, D., and Hart, G.W. (2014). Cross-talk between two essential nutrient-sensitive enzymes: O-GlcNAc transferase (OGT) and AMP-activated protein kinase (AMPK). J Biol Chem *289*, 10592-10606.

Cautain, B., Hill, R., de Pedro, N., and Link, W. (2015). Components and regulation of nuclear transport processes. FEBS J *282*, 445-462.

Cho, D.S., Yang, W., Lee, J.T., Shiekhattar, R., Murray, J.M., and Nishikura, K. (2003). Requirement of dimerization for RNA editing activity of adenosine deaminases acting on RNA. J Biol Chem *278*, 17093-17102.

Christophe, D., Christophe-Hobertus, C., and Pichon, B. (2000). Nuclear targeting of proteins: how many different signals? Cell Signal *12*, 337-341.

Chung, J., Khadka, P., and Chung, I.K. (2012). Nuclear import of hTERT requires a bipartite nuclear localization signal and Akt-mediated phosphorylation. J Cell Sci *125*, 2684-2697.

Cortes, P., Ye, Z.S., and Baltimore, D. (1994). RAG-1 interacts with the repeated amino acid motif of the human homologue of the yeast protein

SRP1. Proc Natl Acad Sci U S A *91*, 7633-7637.

Dong, D.L., and Hart, G.W. (1994). Purification and characterization of an O-GlcNAc selective N-acetyl-beta-D-glucosaminidase from rat spleen cytosol. J Biol Chem *269*, 19321-19330.

Gloster, T.M., Zandberg, W.F., Heinonen, J.E., Shen, D.L., Deng, L., and Vocadlo, D.J. (2011). Hijacking a biosynthetic pathway yields a glycosyltransferase inhibitor within cells. Nat Chem Biol *7*, 174-181.

Goldfarb, D.S., Corbett, A.H., Mason, D.A., Harreman, M.T., and Adam, S.A. (2004). Importin alpha: a multipurpose nuclear-transport receptor. Trends Cell Biol *14*, 505-514.

Gorlich, D., Prehn, S., Laskey, R.A., and Hartmann, E. (1994). Isolation of a protein that is essential for the first step of nuclear protein import. Cell *79*, 767-778.

Gorlich, D., Vogel, F., Mills, A.D., Hartmann, E., and Laskey, R.A. (1995). Distinct functions for the two importin subunits in nuclear protein import. Nature *377*, 246-248.

Haltiwanger, R.S., Blomberg, M.A., and Hart, G.W. (1992). Glycosylation of nuclear and cytoplasmic proteins. Purification and characterization of a uridine diphospho-N-acetylglucosamine:polypeptide beta-N-acetylglucosaminyltransferase. J Biol Chem *267*, 9005-9013.

Hanover, J.A. (2010). Epigenetics gets sweeter: O-GlcNAc joins the "histone code". Chem Biol *17*, 1272-1274.

Hanover, J.A., Yu, S., Lubas, W.B., Shin, S.H., Ragano-Caracciola, M., Kochran, J., and Love, D.C. (2003). Mitochondrial and nucleocytoplasmic isoforms of O-linked GlcNAc transferase encoded by a single mammalian gene. Arch Biochem Biophys *409*, 287-297.

Hu, P., Shimoji, S., and Hart, G.W. (2010). Site-specific interplay between O-GlcNAcylation and phosphorylation in cellular regulation. FEBS Lett *584*, 2526-2538.

Jinek, M., Rehwinkel, J., Lazarus, B.D., Izaurralde, E., Hanover, J.A., and Conti, E. (2004). The superhelical TPR-repeat domain of O-linked GlcNAc transferase exhibits structural similarities to importin alpha. Nat Struct Mol Biol *11*, 1001-1007.

Kamei, Y., Yuba, S., Nakayama, T., and Yoneda, Y. (1999). Three distinct classes of the alpha-subunit of the nuclear pore-targeting complex (importin-alpha) are differentially expressed in adult mouse tissues. J Histochem Cytochem *47*, 363-372.

Khidekel, N., Ficarro, S.B., Clark, P.M., Bryan, M.C., Swaney, D.L., Rexach, J.E., Sun, Y.E., Coon, J.J., Peters, E.C., and Hsieh-Wilson, L.C. (2007). Probing the dynamics of O-GlcNAc glycosylation in the brain using quantitative proteomics. Nat Chem Biol *3*, 339-348.

Kohler, M., Ansieau, S., Prehn, S., Leutz, A., Haller, H., and Hartmann, E. (1997). Cloning of two novel human importin-alpha subunits and analysis of the expression pattern of the importin-alpha protein family. FEBS Lett *417*, 104-108.

Kohler, M., Speck, C., Christiansen, M., Bischoff, F.R., Prehn, S., Haller, H., Gorlich, D., and Hartmann, E. (1999). Evidence for distinct substrate specificities of importin alpha family members in nuclear protein import. Mol Cell Biol *19*, 7782-7791.

Kondoh, K., Terasawa, K., Morimoto, H., and Nishida, E. (2006). Regulation of nuclear translocation of extracellular signal-regulated kinase 5 by active nuclear import and export mechanisms. Mol Cell Biol *26*, 1679-1690.

Kreppel, L.K., Blomberg, M.A., and Hart, G.W. (1997). Dynamic glycosylation of nuclear and cytosolic proteins. Cloning and characterization of a unique O-GlcNAc transferase with multiple tetratricopeptide repeats. J Biol Chem *272*, 9308-9315.

Lazarus, M.B., Nam, Y., Jiang, J., Sliz, P., and Walker, S. (2011). Structure of human O-GlcNAc transferase and its complex with a peptide substrate. Nature *469*, 564-567.

Love, D.C., Kochan, J., Cathey, R.L., Shin, S.H., and Hanover, J.A. (2003). Mitochondrial and nucleocytoplasmic targeting of O-linked GlcNAc transferase. J Cell Sci *116*, 647-654.

Lubas, W.A., Frank, D.W., Krause, M., and Hanover, J.A. (1997). O-Linked GlcNAc transferase is a conserved nucleocytoplasmic protein containing tetratricopeptide repeats. J Biol Chem *272*, 9316-9324.

Ma, J., and Hart, G.W. (2014). O-GlcNAc profiling: from proteins to proteomes. Clin Proteomics *11*, 8.

Nachury, M.V., Ryder, U.W., Lamond, A.I., and Weis, K. (1998). Cloning and characterization of hSRP1 gamma, a tissue-specific nuclear transport factor. Proc Natl Acad Sci U S A *95*, 582-587.

Ozcan, S., Andrali, S.S., and Cantrell, J.E. (2010). Modulation of transcription factor function by O-GlcNAc modification. Biochim Biophys Acta *1799*, 353-364.

Park, S., Jang, I., Zuber, C., Lee, Y., Cho, J.W., Matsuo, I., Ito, Y., and Roth, J. (2014). ERADication of EDEM1 occurs by selective autophagy and requires deglycosylation by cytoplasmic peptide N-glycanase. Histochem Cell Biol *142*, 153-169.

Prieve, M.G., Guttridge, K.L., Munguia, J., and Waterman, M.L. (1998).

Differential importin-alpha recognition and nuclear transport by nuclear localization signals within the high-mobility-group DNA binding domains of lymphoid enhancer factor 1 and T-cell factor 1. Mol Cell Biol *18*, 4819-4832.

Quensel, C., Friedrich, B., Sommer, T., Hartmann, E., and Kohler, M. (2004). In vivo analysis of importin alpha proteins reveals cellular proliferation inhibition and substrate specificity. Mol Cell Biol *24*, 10246-10255.

Roos, M.D., Su, K., Baker, J.R., and Kudlow, J.E. (1997). O glycosylation of an Sp1-derived peptide blocks known Sp1 protein interactions. Mol Cell Biol *17*, 6472-6480.

Ruan, H.B., Nie, Y., and Yang, X. (2013). Regulation of protein degradation by O-GlcNAcylation: crosstalk with ubiquitination. Mol Cell Proteomics *12*, 3489-3497.

Seki, T., Tada, S., Katada, T., and Enomoto, T. (1997). Cloning of a cDNA encoding a novel importin-alpha homologue, Qip1: discrimination of Qip1 and Rch1 from hSrp1 by their ability to interact with DNA helicase Q1/RecQL. Biochem Biophys Res Commun *234*, 48-53.

Shevchenko, A., Tomas, H., Havlis, J., Olsen, J.V., and Mann, M. (2006). In-gel digestion for mass spectrometric characterization of proteins and proteomes. Nat Protoc *1*, 2856-2860.

Slawson, C., Housley, M.P., and Hart, G.W. (2006). O-GlcNAc cycling: how a single sugar post-translational modification is changing the way we think about signaling networks. J Cell Biochem *97*, 71-83.

Tai, H.C., Khidekel, N., Ficarro, S.B., Peters, E.C., and Hsieh-Wilson, L.C. (2004). Parallel identification of O-GlcNAc-modified proteins from cell lysates. J Am Chem Soc *126*, 10500-10501.

Torres, C.R., and Hart, G.W. (1984). Topography and polypeptide distribution of terminal N-acetylglucosamine residues on the surfaces of intact lymphocytes. Evidence for O-linked GlcNAc. J Biol Chem *259*, 3308-3317.

Tsuji, L., Takumi, T., Imamoto, N., and Yoneda, Y. (1997). Identification of novel homologues of mouse importin alpha, the alpha subunit of the nuclear pore-targeting complex, and their tissue-specific expression. FEBS Lett *416*, 30-34.

Valente, L., and Nishikura, K. (2007). RNA binding-independent dimerization of adenosine deaminases acting on RNA and dominant negative effects of nonfunctional subunits on dimer functions. J Biol Chem *282*, 16054-16061.

Weis, K., Mattaj, I.W., and Lamond, A.I. (1995). Identification of hSRP1 alpha as a functional receptor for nuclear localization sequences. Science *268*, 1049-1053.

Wells, L., Vosseller, K., and Hart, G.W. (2001). Glycosylation of nucleocytoplasmic proteins: signal transduction and O-GlcNAc. Science *291*, 2376-2378.

Wells, L., Whelan, S.A., and Hart, G.W. (2003). O-GlcNAc: a regulatory post-translational modification. Biochem Biophys Res Commun *302*, 435-441.

Whelan, S.A., Lane, M.D., and Hart, G.W. (2008). Regulation of the O-linked beta-N-acetylglucosamine transferase by insulin signaling. J Biol Chem *283*, 21411-21417.

Xu, L., Alarcon, C., Col, S., and Massague, J. (2003). Distinct domain utilization by Smad3 and Smad4 for nucleoporin interaction and nuclear import. J Biol Chem *278*, 42569-42577.

Xu, L., and Massague, J. (2004). Nucleocytoplasmic shuttling of signal transducers. Nat Rev Mol Cell Biol *5*, 209-219.

Yuzwa, S.A., Shan, X., Macauley, M.S., Clark, T., Skorobogatko, Y., Vosseller, K., and Vocadlo, D.J. (2012). Increasing O-GlcNAc slows neurodegeneration and stabilizes tau against aggregation. Nat Chem Biol *8*, 393-399.

Chapter 3

X-linked Inhibitor of Apoptosis Protein (XIAP) Promotes Degradation of OGT and Inhibits Cancer Cell Growth

1. Abstracts

O-GlcNAcylation and *O*-GlcNAc transferase (OGT) levels are elevated in many cancer types. Increased *O*-GlcNAcylation plays an important roles in key metabolic and signaling pathways that conduct multiple cancer phenotypes. However, little is known about how subcellular OGT protein levels are regulated. Here, We report that X-linked inhibitor apoptosis protein (XIAP), a well-known caspase inhibitor, is *O*-GlcNAcylated and directly ubiquitylates and promotes proteasomal-dependent degradation of OGT. *O*-GlcNAc modification at Ser406 reduces its E3 ligase activity for OGT. The HCT116 human colorectal carcinoma cells stably overexpressing XIAP show reduced OGT protein level and cancer cell growth. Our study reveals an antigrowth function of XIAP which suppresses tumorigenesis.

2. Introduction

X-linked inhibitor of apoptotic protein (XIAP; also known as BIRC4) is characterized a member of the IAP family and a compelling inhibitor of the caspase mediated apoptosis pathway (Srinivasula and Ashwell, 2008). XIAP possesses three N-terminal baculovirus IAP repeat (BIR) domains, which together with flanking residues, can bind directly to caspases 3, 7, and 9 and a C-terminal really interesting new gene (RING) domain, which participates in the ubiquitin-proteasome pathway through their roles as E3 ubiquitin ligases (Joazeiro et al., 2000; Schimmer et al., 2006). The UBA domain in XIAP and a RING dimerization are important for the XIAP's ability to bind K63-linked poly-ubiquitin, and in some cases to K48-linked poly-ubiquitin (Gyrd-Hansen et al., 2008). XIAP ubiquitinates a broad range of cellular substrates, thereby participating in a range of cellular activities beyond anti-apoptotic effects (Galban and Duckett, 2010; Srinivasula and Ashwell, 2008). Although XIAP is reportedly shown as acting a role in promoting cancer invasion and metastasis, some conflicting data also exist. This has been a challenge in understanding how XIAP can be such a versatile, multi-functional protein related to cancer cell biology.

O-linked *N*-acetylglucosamine (*O*-GlcNAc) occurs on hydroxyl groups of serine or threonine residue, like phosphorylation (Wells et al., 2001). *O*-GlcNAc modification is controlled by *O*-GlcNAc transferase (OGT) in the nucleus and cytoplasm (Haltiwanger et al., 1992). OGT transfers beta *N*-acetylglucosamine from UDP-GlcNAc to target proteins that are participated in various biological processes, including protein-protein interactions, epigenetic regulation, protein stability, localization, and enzyme activity (Butkinaree et al., 2010; Love and Hanover 2005; Zachara and Hart 2004).

Numerous reports suggest that many cellular proteins are abnormally

O-GlcNAc modified in many types of cancer (Lynch and Reginato, 2011; Slawson and Hart, 2011), such as bladder cancer (Rozanski et al., 2012), colorectal and lung cancer (Mi et al., 2011), pancreatic cancer (Ma et al., 2013), and prostate cancer (Lynch et al., 2012). Increasing OGT and *O*-GlcNAc during breast cancer progression are correlated with the histological grade of the tumor (Caldwell et al., 2010; Krzeslak et al., 2012), suggesting OGT plays a critical role in tumorigenesis. Although OGT protein level is maintained at a high status, little is known about the mechanisms of OGT protein regulation in cancer cells.

Here, we report that XIAP functions as an E3 ligase and promotes the proteasome-dependent degradation of OGT in vitro and in vivo. XIAP also might undergo *O*-GlcNAc modification at Ser406 and the modification of XIAP influences on its E3 ligase activity for OGT. The HCT116 human colorectal carcinoma cells stably overexpressing XIAP showed reduced cell proliferations. Our study suggest novel function of XIAP in the regulation of cancer cell growth, which is distinctly different from its well-characterized apoptotic suppression.

3. Material and Methods

Cell culture, DNA transfection and plasmids

HEK293, Human colon cancer cell lines HCT116 wild-type and XIAP -/- HCT116 cells, and breast cancer cell lines MDA-MB231 cells were cultured in Dulbecco's Modified Eagle's Medium (Lonza, Basel, Swiss) supplemented with 10% fetal bovine serum, 100 U/ml penicillin and 100 μg/ml streptomycin at 37°C in 5% CO2. DNA was transfected using polyethylenimine (Sigma-Aldrich, St Louis, MO) as described previously (Boussif et al., 1995). Human OGT, wild-type XIAP, and mutant S406A XIAP were cloned into the p3xFLAG-CMVTM-7.1 ExpressionVector (Sigma-Aldrich, St Louis, MO). Human wild-type XIAP and ΔRING XIAP proteins were cloned into pRK5 in frame with an N-terminal Myc epitope. The mutant S406A XIAP was generated using the QuikChange Site-Directed Mutagenesis Kit (Stratagene, La Jolla, CA). The mutations was confirmed by DNA sequence analysis. To generate GST-tagged OGT, the cDNA encoding full-length OGT was cloned downstream of the GST coding sequence in pGEX-5X (Clontech, Rockville, MD). His-tagged wild-type XIAP and mutant S406A XIAP were cloned into pET6xHN expression vector (Clontech, Rockville, MD).

Reagent and antibodies

Antibodies against XIAP (H-202, rabbit polyclonal), HA (Y-11, rabbit polyclonal), Myc (B-14, mouse monoclonal), GST (9E10, mouse monoclonal, Santa Cruz), α-tubulin (TU-02, mouse monoclonal), β-actin (C-2, mouse monoclonal), GAPDH (6C5, mouse monoclonal) were purchased from Santa Cruz, Dallas, Texas. Antibodies against Flag (F-3156, mouse monoclonal) and OGT (DM17, rabbit polyclonal) were from Sigma-Aldrich, St Louis, MO. CTD110.6, an antibody against

O-GlcNAc, was purchased from Covance (Princeton, NJ). E1 (UBE1, E1-305) and E2 (UbcH5c, E2-627) were purchased from Boston Biochem.

sWGA affinity purification, immunoprecipitation and Western blotting

HEK293 cells were lysed with NET lysis buffer (150 mM NaCl, 50 mM Tris, pH 7.4, 1 mM EDTA, 1% Nonidet P-40) supplemented with a protease inhibitor cocktail (Roche, Mannheim, Germany) and cell lysates were incubated with agarose-conjugated succinylated wheat germ agglutinin (sWGA, Vector Laboratories, Burlingame, CA) for 3 h at 4°C. For control of specificity, 20 mM GlcNAc was added. Precipitates were washed 4 times with lysis buffer and protein were eluted by boiling in SDS sample buffer. Immunoprecipitation and Western blotting are described previously (Seo et al., 2016).

In vivo and in vitro Ubiquitylation Assay

HEK293 cells were transiently co-expressed with Flag-tagged OGT, Myc-tagged XIAP, and HA-tagged ubiquitin for in vivo in vitro ubiquitylation. After 48 h of transfection, cells were treated with MG132 (20 μM) for 2 h and then harvested with RIPA buffer supplemented with aprotinin (10 μg/μl), leupeptin (10 μg/μ), DTT (1 mM), and ubiquitin aldehyde (5 μM). The cell extracts were subjected to immunoprecipitation using Flag antibody-conjugated A/G beads or pull-down with Glutathione-Sepharose4B (GE Healthcare) beads under denature condition with buffer containing 2% SDS. The beads were washed three times with RIPA buffer followed by SDS-PAGE. For OGT in vitro ubiquitylation, 2 μg GST-OGT and 300 ng His-XIAP (purified) were incubated with 150 ng E1 (UBE1), 400 ng E2 (UbcH5c), and 5 μg HA-ubiquitin in 50 μl volumes containing 25 mM Tris-HCl (pH 8.0), 4 mM ATP, 5 mM MgCl2, 200 μM CaCl2, and 1 mM DTT.

After incubation in 37°C for 2h GST-OGT proteins were pulled down by GST beads. These beads were washed three times with corresponding buffer, and the immobilized proteins were subjected to SDS-PAGE. The ubiquitylation of OGT was analyzed by immunoblotting with HA antibody.

Quantitative real-time PCR

Total RNA was isolated from HEK293 cells using TRIzol reagent (Invitrogen). Complementary DNA was synthesized using ReverTra Ace qPRC RT Master Mix (Toyobo Co., Japan). Quantitative real-time PCR was performed using SYBR Premix Ex Taq (Takara, Japan). All reactions were done according to manufacturer's instructions. Amplified product was analyzed by Applied Biosystems 7300 Real-Time PCR system. Gene specific primers were as follows:

OGT, forward 5′-CTTTAGCACTCTGGCAATTAAACAG-3′,

OGT, reverse 5′-TCAAATAACATGCCTTGGCTTC-3′

GAPDH, forward 5′-AGGGCTGCTTTTAACTCTGGT-3′,

GAPDH, reverse 5′-CCCCACTTGATTTTGGAGGGA-3′.

The mRNA levels of OGT were normalized to GAPDH.

Stable cell line establishment

XIAP were cloned into retroviral vector pMSCV-Flag for stable cells establishment. Together with retroviral packaging plasmids pVSV-G and Gag/Pol, 3 μg retroviral DNA constructs were transfected into 293T cells. Retroviral particles were collected twice at 24 h and 48 h after transfection to infect target cells supplement with 10 μg/ml final concentration polybrene. After 24 h of infection, start to antibiotic selection till get the stable transgenic cells.

Cell counting

HCT116 cells were seeded in 60-mm dishes, 10 x 104 cells per plate. After treatment the cells were incubated with 0.25% Trypsin-EDTA (Gibco) for 1 min and then harvested. The cells were re-suspended in 25mM Dulbecco's Modified Eagle's Medium. 1:1 ratio diluted cells were prepared by mixing with 0.4% Trypan blue stain (Gibco) and incubating for 5 min. The stained cells were then transferred to a Neubauer improved chamber (Marienfeld) and viable cells were counted under OLYMPUS CK2-TRC microscope. The number of cells in 0.1 µl of cells were obtained by counting four large squares, then dividing the sum of the four cells by 4, and multiplying by dilution factor 2. The number of cells per ml was obtained by multiplying the cell number from the previous calculation with 10^4.

4. Results

4.1. XIAP is modified by *O*-GlcNAc

Various studies demonstrate that maintaining elevated OGT and *O*-GlcNAcylation levels are important for cancer cell progression (Fardini et al., 2013; Lynch and Reginato, 2011). Since it has been reported that the correlation between abnormal X-linked inhibitor of apoptosis protein (XIAP) expression and malignant cancer progression (Fong et al., 2000; Yang et al., 2003), we first addressed the question of whether XIAP could be a substrate of OGT. To examine whether endogenous XIAP is modified by *O*-GlcNAc, we used succinylated wheat germ agglutinin (sWGA) for affinity purification of HEK293 total cell lysates (Gambetta et al., 2009; Love and Hanover, 2005) and probed the precipitates with an antibody against XIAP. We successfully detected *O*-GlcNAc modified endogenous XIAP (Figure 1A). The specificity of the lectin affinity purification was demonstrated by addition of the inhibitory mono-saccharide GlcNAc (Figure 1A). Next, human XIAP were cloned into the Flag-tagged expression vector and transiently expressed in HEK293 cells. Immunoprecipitated Flag-tagged XIAP was probed with the *O*-GlcNAc-specific antibody. We were able to unequivocally detect *O*-GlcNAc on XIAP in an amount which could be significantly increased by co-expressed OGT, and decreased by co-expressed OGA (Figure 1B). To determine the existence and location of the *O*-GlcNAc site(s) on XIAP by mass spectrometry analysis, XIAP was immunoprecipitated from HEK293 cells co-expressing OGT and subjected to SDS-PAGE. The precipitated XIAP was then in-gel digested with trypsin, and analyzed by quadrupole time-of-flight tandem mass spectrometry (Q-TOF MS). The *O*-GlcNAc modified 406-419 peptide of XIAP was observed (data not shown). Since there is only one serine residue in XIAP 406-419 peptide, we were able to conclude

that serine 406 might be *O*-GlcNAc modified. We created a site-specific point mutant of XIAP. Mutation of Ser406 with alanine showed a completely disappeared *O*-GlcNAc modification (Figure 1C). Next, to rule out the possibility that the substitution alanine for Ser406 in XIAP does not affect its functional protein-protein interaction with OGT, co-immunoprecipitation was performed. Both wild-type XIAP and S406A XIAP interacted with OGT (Figure 1D-E). The XIAP RING domain has E3 ubiquitin ligase activity and is able to associate with other proteins when XIAP is transiently overexpressed. To examine whether the binding between XIAP and OGT is functional not due to XIAP's RING domain, deletion mutant of XIAP lacked the C-terminal RING domain was used. The deletion mutant XIAP lacking RING domain still interacted with OGT (Figure 1F). Taken together, these results indicate that XIAP is *O*-GlcNAcylated, may be at Ser406 residue and has a functional interaction with OGT.

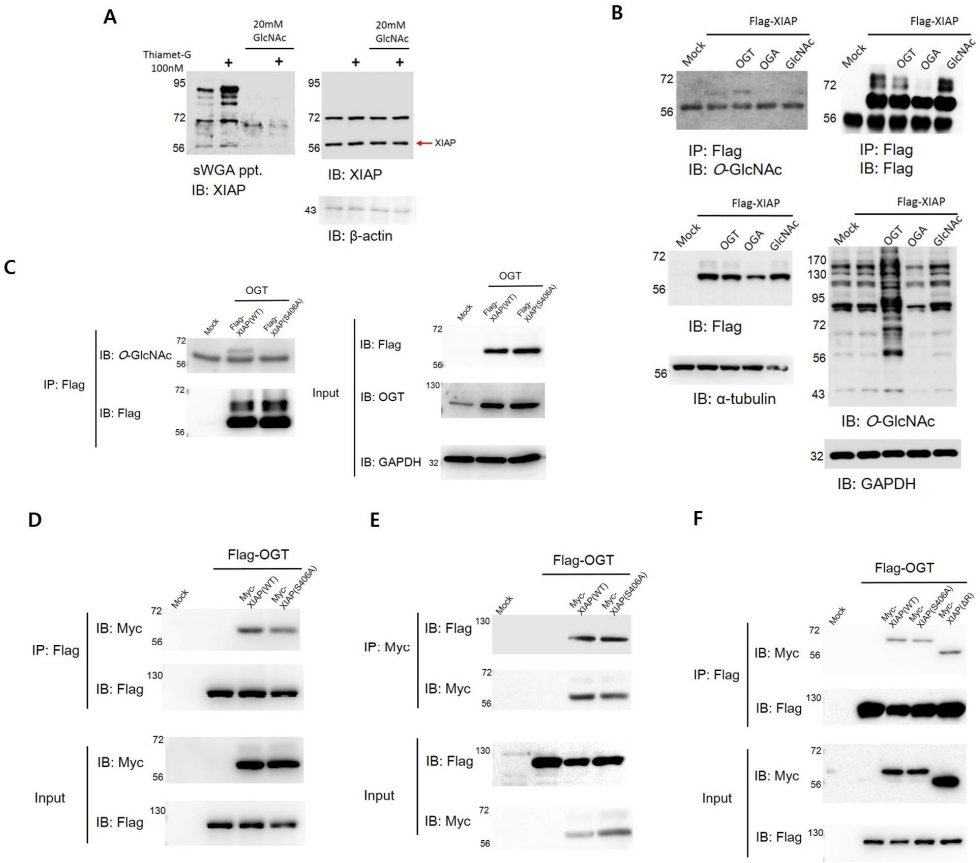

Figure 1. XIAP carries *O*-GlcNAc modification at Ser406

(A) HEK293 cells were treated with Thiamet-G (100 nM, 4 h) and cell lysates were subjected to sWGA lectin affinity purification and the precipitates analyzed with Western blot for endogenous XIAP. For control, mono-saccharide inhibitor GlcNAc (20 mM) was added during sWGA lectin affinity purification.

(B) Western blot analysis for *O*-GlcNAc of immunoprecipitated XIAP from transiently overexpressing OGT, OGA, or control vector transfected HEK293 cells. Blotting with an α-Flag antibody confirmed that equal amounts of the XIAP constructs were immunoprecipitated.

(C) Flag-tagged WT-XIAP or XIAP point mutants were transfected in transiently overexpressing OGT HEK293 cells. WT-XIAP and XIAP point mutants were immunoprecipitated with an α-Flag antibody and blotted with an α-*O*-GlcNAc antibody.

(D) HEK293 cells transiently overexpressing Myc-tagged WT-XIAP or XIAP S406A mutant together with Flag-tagged OGT were immunoprecipitated with an α-Flag antibody and the beads were stringently washed three times. Co-immunoprecipitated XIAP constructs were detected by an α-Myc antibody. Blotting with an α-Myc antibody revealed that equal amounts of XIAP were immunoprecipitated.

(E) HEK293 cells were transfected as in (D) were immunoprecipitated with an α-Myc antibody. . Co-immunoprecipitated OGT constructs were blotted with an α-Flag antibody. An α-Myc antibody immunoblotting confirmed that equal amounts of XIAP were immunoprecipitated.

(F) Myc-tagged WT-XIAP, XIAP S406A mutant, or XIAP ΔR mutant were transfected transiently overexpressing Flag-tagged OGT HEK293 cells. Cell lysates were immunoprecipitated with an α-Flag antibody. Co-immunoprecipitated XIAP as well as the loading amounts were analysed by western blotting with an α-Flag antibody. An α-Myc antibody immunoblotting confirmed that equal amounts of XIAP constructs were immunoprecipitated.

4.2. OGT is a substrate of the E3 ligase XIAP in vitro and in vivo

The finding that XIAP is *O*-GlcNAcylated and interacts with OGT prompted us to investigate whether XIAP could ubiquitylate OGT in vivo. Expression vectors encoding Flag-OGT and HA-Ub were co-transfected into HEK293 cells transiently expressing Myc-XIAP. As shown in Figure 2A, the ubiquitylation of OGT was largely increased in Myc-XIAP transiently expressing HEK293 cells compared with only OGT transfected cells. To determine whether XIAP could ubiquitylate OGT in vitro, pull-down experiments were performed in which glutathione S-transferase (GST)-OGT fusion protein was incubated with His-tagged XIAP fusion protein under denatured condition with buffer containing 2% SDS. As expected, poly-ubiquitylation of GST-tagged OGT was observed, whereas without His-tagged XIAP showed no detectable ubiquitylation (Figure 2B). We next performed similar in vivo ubiquitylation assay in HCT116 wild type (WT) and HCT116 XIAP-deficient (XIAP-/-) cells. Decreased ubiquitylation of OGT was observed in HCT116 XIAP-/- cells compared with HCT WT cells (Figure 2C). Taken together, the results show that XIAP is an E3 ubiquitin ligase and ubiquitylates OGT in vivo and in vitro.

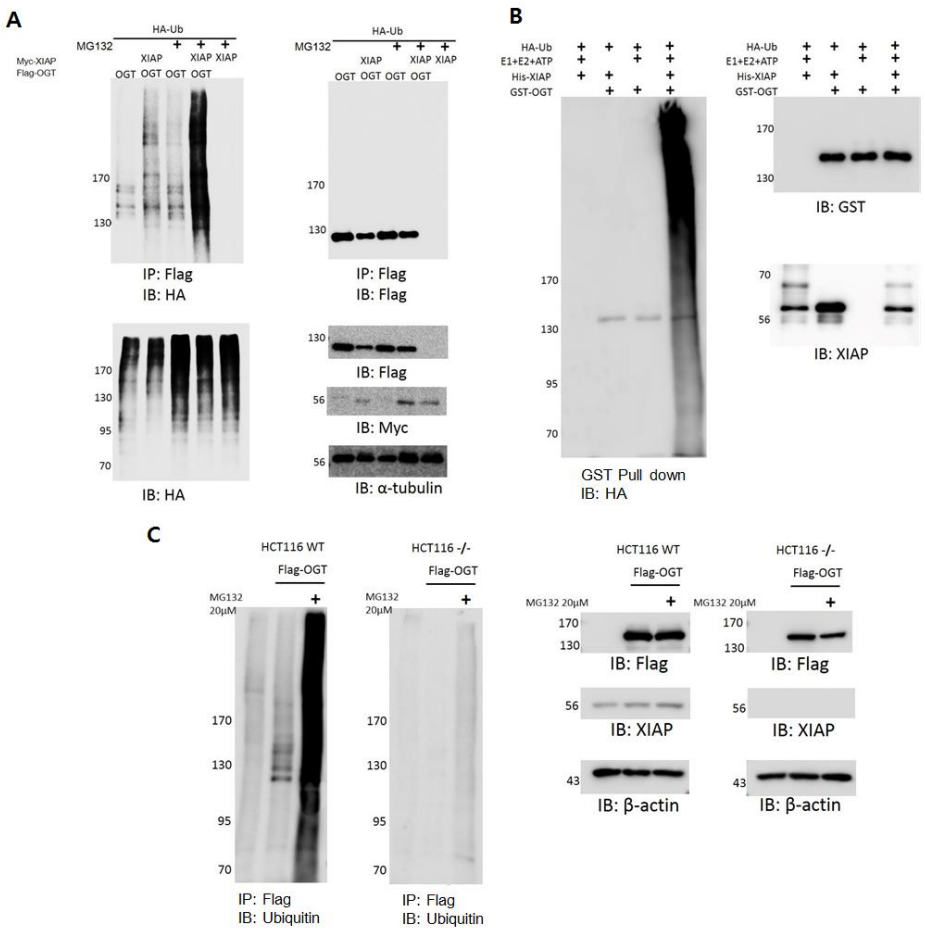

Figure 2. XIAP acts as an E3 ligase of OGT

(A) The expression vector encoding Flag-tagged OGT and HA-Ub were transfected into HEK293 cells, which transiently overexpressing Myc-tagged XIAP as indicated. After immunoprecipitation by an α-Flag antibody, the ubiquitylation of OGT was analyzed by immunoblotting with an α-HA antibody. Equal amounts of whole cell lysates were subjected to immunoblotting with antibodies as indicated.

(B) GST-OGT was incubated with His-XIAP, HA-ubiquitin, E1, E2, and ATP as indicated. After GST pull-down under denature condition

with buffer containing 2% SDS. The ubiquitylation of OGT was analyzed by immunoblotting with an α-HA antibody. The same amounts of OGT in the reaction was immunoblotted with an α-GST antibody.

(C) HCT116 WT or HCT116 XIAP-/- cells were transfected with Flag-tagged OGT and were then treated with MG132 (20 μM) for 2 h. The ubiquitylation of immunoprecipitated OGT was analyzed by immunoblotting with an α-ubiquitin antibody.

4.3. XIAP induced degradation of OGT

Protein ubiquitylation is known to regulate protein degradation and subcellular signaling. To investigate the function of XIAP-mediated ubiquitylation of OGT, we measured the half-lives of OGT in HCT116 wild type (WT) and HCT116 XIAP-deficient (XIAP-/-) cells in the presence of CHX. The protein level of OGT decreased at a much slower rate in XIAP-/- cells than in XIAP WT cells (Figure 3A), whereas the mRNA levels of OGT in the two cell lines were comparable (Figure 3B). Thus, our results suggest that the turnover of OGT is regulated at protein level, possibly through an ubiquitin-dependent pathway. We next transfected Flag-tagged XIAP into HEK293 cells and measured the protein level of endogenous OGT in the presence or absence of MG132. In support of our hypothesis, XIAP-mediated degradation of OGT was blocked by the addition of MG132 (Figure 3C-D). No significant difference of mRNA levels was observed in transiently overexpressing Flag-tagged XIAP cells treated with MG132 or not treated (Figure 3E). Collectively, the results indicate that XIAP promotes proteasomal-dependent degradation of OGT in vivo.

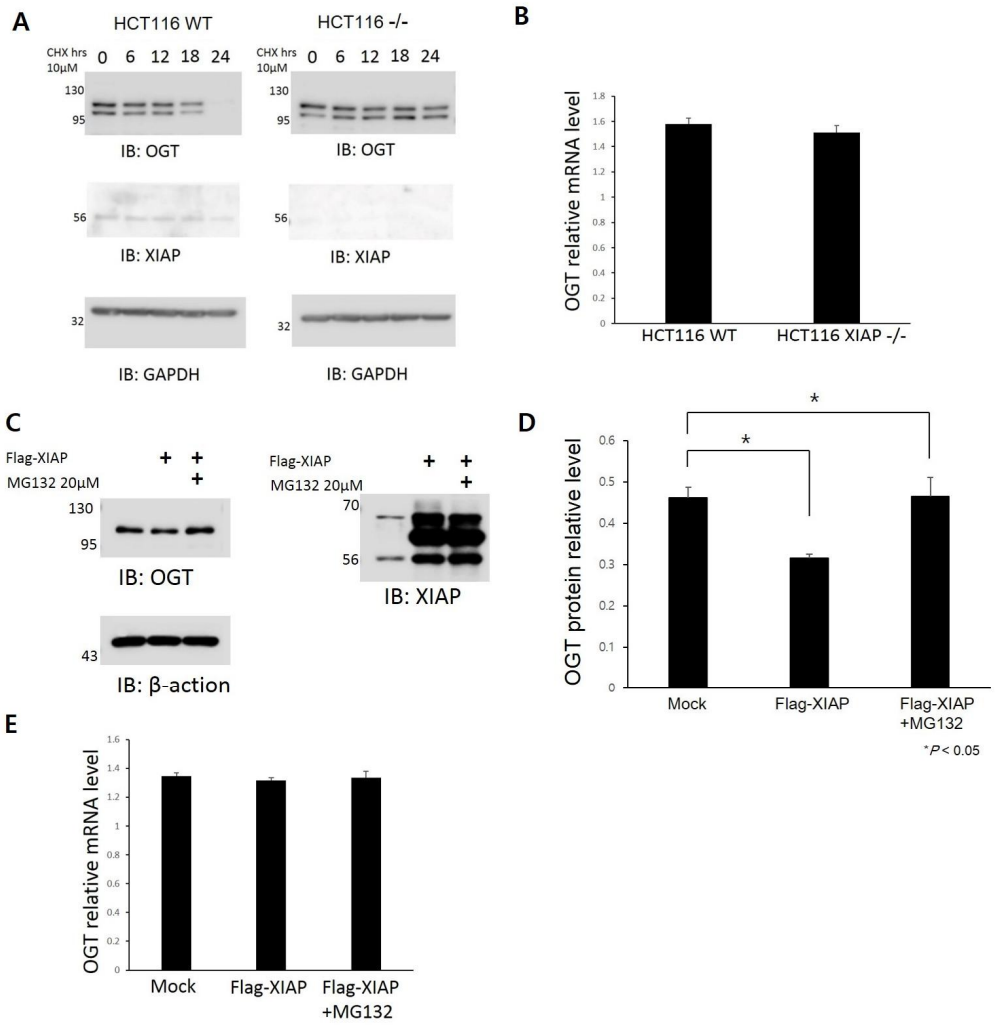

Figure 3. XIAP promotes OGT protein degradation

(A) HCT116-WT or HCT116 XIAP -/- cells were treated with CHX (10 μM) and harvested at the indicated time points. The expression levels of OGT, XIAP and GAPDH were determined by immunoblotting.

(B) OGT mRNA levels in HCT116-WT or HCT116 XIAP -/- cells were measured by qRT-PCR. The value was normalized by GAPDH mRNA levels. The error bars represent ± s.d.,; triplicate experiments.

(C-D) The empty vector or the expression vector encoding Flag-tagged XIAP was transfected into HEK293 cells as indicated. Before harvest, the cells were treated with or without MG132 (20 μM) as indicated. The expression levels of OGT, XIAP, and β-actin were determined (A), and the relative protein level of OGT was quantified (B).

(E) HEK93 cells were prepared as in (A). The mRNA levels of OGT were detected by qRT-PCR. GAPDH was used for normalization. The error bars represent ± s.d.,; triplicate experiments.

4.4 *O*-GlcNAc modification at Ser406 plays an important role in E3 ligase activity of XIAP

It has been verified that the Ser406 residue of XIAP is located in the ubiquitin associated (UBA) domain. Since the presence of the UBA domain in XIAP is essential for XIAP's ability to bind K63-linked poly-ubiquitin and in some cases to K48-linked poly-ubiquitin (Gyrd-Hansen et al., 2008), we next speculated that *O*-GlcNAc modification of XIAP influence on the XIAP mediated ubiquitylation of OGT. To determine whether Ser406 *O*-GlcNAc modification on XIAP is important for poly-ubiquitylation of OGT, purified glutathione S-transferase (GST)-OGT fusion protein was incubated with HEK293 transiently overexpressing Flag-tagged wild-type XIAP or Flag-tagged S406A mutant XIAP, respectively. Upon pull-down of OGT with GST beads and immunoblotting with an anti-HA antibody to detect ubiquitin, we observed that GST-OGT with Myc-tagged wild-type XIAP showed an apparent large mobility shift, indicating an efficient poly-ubiquitylation of OGT compared to Myc-tagged S406A mutant XIAP (Figure 4A). The finding was further confirmed in an in vitro ubiquitylation assay, in which GST-OGT was efficiently ubiquitylated by His-tagged wild-type XIAP fusion protein but not His-tagged S406A mutant XIAP fusion protein (Figure 4B). These results presumably indicate that Ser406 *O*-GlcNAc modification in XIAP may affect the E3 ligase activity of XIAP.

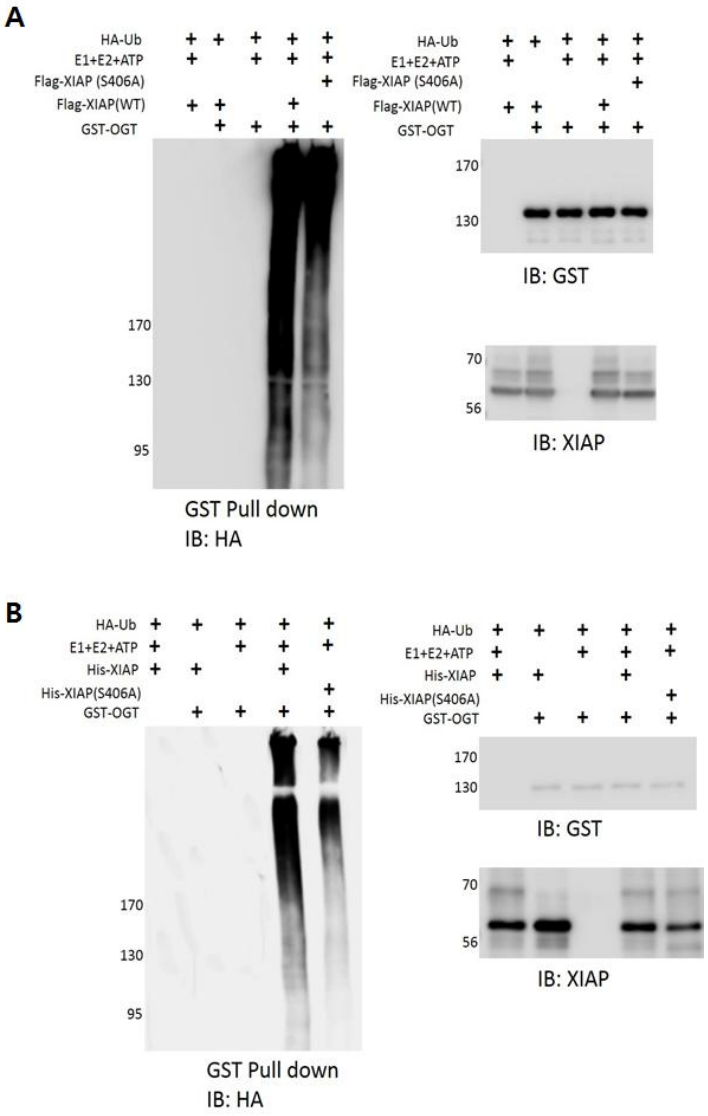

Figure 4. Mutation of XIAP reduced its E3 ligase activity for OGT

(A) The expression vector encoding Flag-tagged XIAP (WT) or Flag-tagged XIAP (S406A) were transfected into HEK293 cells as indicated. Cell lysates were then incubated with GST-OGT,

HA-Ubiquitin, E1, E2, and ATP as indicated. After pull-down by GST beads, the ubiquitylation of OGT was analyzed by immunoblotting with an α-HA antibody. Equal amounts of whole cell lysates were subjected to immunoblotting with antibodies as indicated.

(B) GST-OGT was incubated with His-XIAP (WT) or His-XIAP (S406), together with HA-Ubiquitin, E1, E2, and ATP as indicated. After GST pull-down under denature condition with buffer containing 2% SDS, the ubiquitylation of OGT was detected by immunoblotting with an α-HA antibody. The amounts of OGT in the reaction were immunoblotted with an α-GST antibody.

4.5 XIAP inhibits HCT11.6 cell growth through degradation of OGT

OGT is overexpressed in various cancer cells and plays an important role in cell growth (Lynch and Reginato, 2011). XIAP also atypically exhibits deregulated protein levels because of resistance to anti-cancer drugs by binding to and suppressing caspase function (Schimmer et al., 2006). To verify the role of OGT and XIAP in cancer cells, first we established different cancer cell lines stably expressing XIAP, such as adenocarcinomic human alveolar basal epithelial cells (A549), human breast adenocarcinoma cells (MDA-MB-231), human colorectal carcinoma cells (HCT116) Wild-type, and HCT116 XIAP -/- cells. As shown in Figure 5A, OGT and total *O*-GlcNAcylation levels were reduced in stably overexpressing Flag-tagged XIAP HCT116 cells compared to control HCT116 cells. Next, we performed a cell proliferation assay . The introduction of XIAP gene by infection with Flag-XIAP retroviral particles in HCT116 cells showed the phenomenon of decreased cell growth (Figure 5B). Collectively, these data suggest that abnormally overexpressed XIAP induced the degradation of OGT protein levels and consequently disrupted cancer cell growth rate.

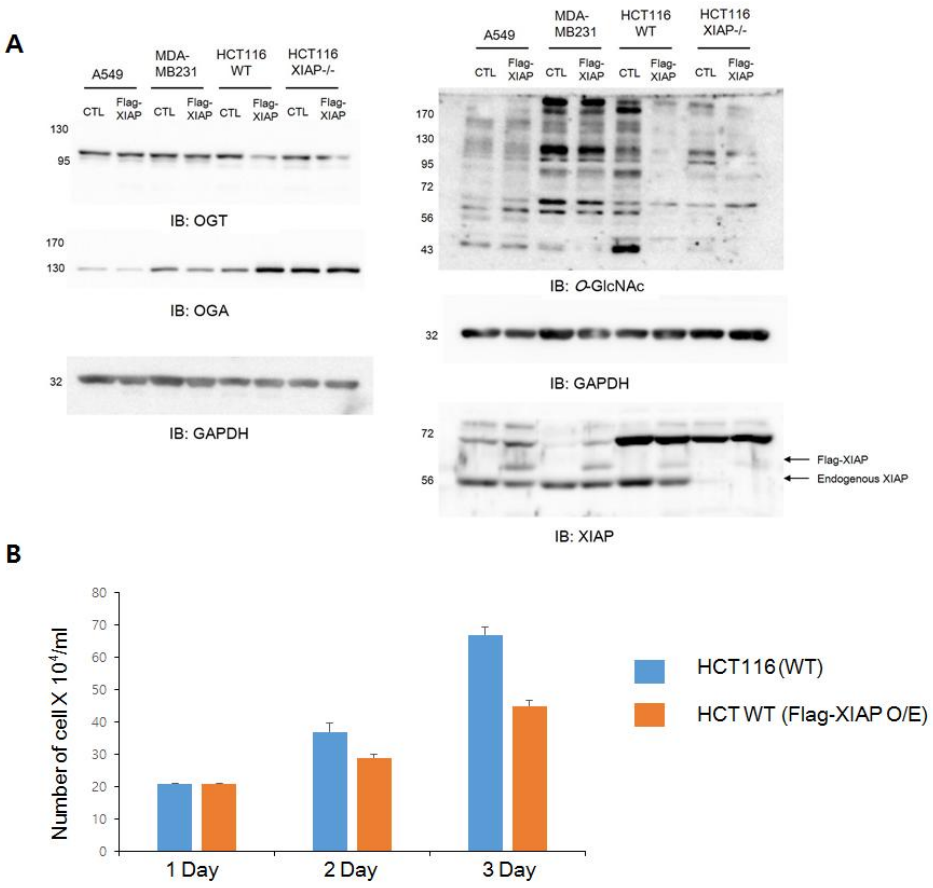

Figure 5. XIAP inhibits HCT116 colorectal carcinoma cell growth by inducing the degradation of OGT

(A) Establishing of A549, MDA-MB231, HCT116(WT), and HCT116(XIAP-/-) overexpressing Flag-tagged XIAP cell lines by introducing retroviral particle packaging. Total cell lysates was immunoblotted as indicated antibodies, respectively .

(B) HCT116 (WT) and HCT116 (Flag-XIAP O/E) cells were treated with trypsin and counted using 0.4% Trypan blue staining and a Neubauer improved counting chamber. The value indicates number of cells per ml.

4. Discussion

O-linked *N*-acetylglucosamine (*O*-GlcNAc) is a post-translational modification on hydroxyl groups of serine or threonine residues of nuclear and cytoplasmic proteins (Wells et al., 2001). *O*-GlcNAcylation plays crucial regulatory roles in various cellular signaling processes (Hanover, 2010; Ozcan et al., 2010; Roos et al., 1997; Ruan et al., 2013; Slawson et al., 2006; Wells et al., 2003). Recent works in many different cancer types now indicate that abnormally increased OGT and *O*-GlcNAcylation levels are a general feature of cancer and contribute to transformed cancer phenotypes (Ferrer et al., 2014; Itkonen et al., 2016; Lynch et al., 2012). Although known for XIAP's ability to inhibit caspase and apoptosis, XIAP also participated in other diverse subcellular functions, including copper metabolism, signal activation, and ubiquitination (Eckelman et al., 2006). Here, we found that OGT interacts with XIAP and *O*-GlcNAcylated XIAP at Ser406 (Figure 1 A-C). The interaction between XIAP and OGT is functional because substitution of Alanine for Serine 406 also binds to OGT (Figure 1D-E). Given that XIAP has been known to exhibit ubiquitin protein ligase activity (E3 ligase) (Suzuki et al., 2001), we assessed whether XIAP was prompting OGT degradation in the proteasome through ubiquitin dependent pathway. We observed XIAP mediated ubiquitylation of OGT (Figure 2A-C) and degradation in the proteasome (Figure 3A-E). So far, the ubiquitin associated (UBA) domain in the IAP family proteins has been lately characterized (Gyrd-Hansen et al., 2008). The mechanisms how UBA domain in XIAP lead to recognize and interact with poly-ubiquitin chain remain unclear. Since *O*-GlcNAc modification occurs on Ser406 of XIAP where UBA domain (residues 368-419) is located, we investigate XIAP's E3 ligase activity for OGT. The mutation of *O*-GlcNAcylation Ser406 in XIAP results in decreased OGT's poly- ubiquitylation (Figure 4 A-B). Next, stably overexpressing

XIAP colorectal carcinoma cell lines (HCT116) were established to further investigate the role of OGT and XIAP in cancer cells. Overexpressed XIAP induced degradation of OGT and total *O*-GlcNAcylation levels (Figure 5A) and inhibited HCT116 cancer cell growth (Figure 5B). These studies collectively support the hypothesis that abnormal expression of XIAP inhibits the growth of certain type of tumors, in which the elevated level of OGT upon perhaps the loss of XIAP is required for cancer cell growth and proliferation. Our study may expand XIAP′s role in tumor growth through degradation of OGT.

5. References

Butkinaree, C., Park, K., and Hart, G.W. (2010). O-linked beta-N-acetylglucosamine (O-GlcNAc): Extensive crosstalk with phosphorylation to regulate signaling and transcription in response to nutrients and stress. Biochim Biophys Acta 1800, 96-106.

Caldwell, S.A., Jackson, S.R., Shahriari, K.S., Lynch, T.P., Sethi, G., Walker, S., Vosseller, K., and Reginato, M.J. (2010). Nutrient sensor O-GlcNAc transferase regulates breast cancer tumorigenesis through targeting of the oncogenic transcription factor FoxM1. Oncogene 29, 2831-2842.

Champattanachai, V., Netsirisawan, P., Chaiyawat, P., Phueaouan, T., Charoenwattanasatien, R., Chokchaichamnankit, D., Punyarit, P., Srisomsap, C., and Svasti, J. (2013). Proteomic analysis and abrogated expression of O-GlcNAcylated proteins associated with primary breast cancer. Proteomics 13, 2088-2099.

Eckelman, B.P., Salvesen, G.S., and Scott, F.L. (2006). Human inhibitor of apoptosis proteins: why XIAP is the black sheep of the family. EMBO Rep 7, 988-994.

Fardini, Y., Dehennaut, V., Lefebvre, T., and Issad, T. (2013). O-GlcNAcylation: A New Cancer Hallmark? Front Endocrinol (Lausanne) 4, 99.

Ferrer, C.M., Lynch, T.P., Sodi, V.L., Falcone, J.N., Schwab, L.P., Peacock, D.L., Vocadlo, D.J., Seagroves, T.N., and Reginato, M.J. (2014). O-GlcNAcylation regulates cancer metabolism and survival stress signaling via regulation of the HIF-1 pathway. Mol Cell 54, 820-831.

Fong, W.G., Liston, P., Rajcan-Separovic, E., St Jean, M., Craig, C., and

Korneluk, R.G. (2000). Expression and genetic analysis of XIAP-associated factor 1 (XAF1) in cancer cell lines. Genomics 70, 113-122.

Galban, S., and Duckett, C.S. (2010). XIAP as a ubiquitin ligase in cellular signaling. Cell Death Differ 17, 54-60.

Gambetta, M.C., Oktaba, K., and Muller, J. (2009). Essential role of the glycosyltransferase sxc/Ogt in polycomb repression. Science 325, 93-96.

Gyrd-Hansen, M., Darding, M., Miasari, M., Santoro, M.M., Zender, L., Xue, W., Tenev, T., da Fonseca, P.C., Zvelebil, M., Bujnicki, J.M., et al. (2008). IAPs contain an evolutionarily conserved ubiquitin-binding domain that regulates NF-kappaB as well as cell survival and oncogenesis. Nat Cell Biol 10, 1309-1317.

Haltiwanger, R.S., Blomberg, M.A., and Hart, G.W. (1992). Glycosylation of nuclear and cytoplasmic proteins. Purification and characterization of a uridine diphospho-N-acetylglucosamine:polypeptide beta-N-acetylglucosaminyltransferase. J Biol Chem 267, 9005-9013.

Hanover, J.A. (2010). Epigenetics gets sweeter: O-GlcNAc joins the "histone code". Chem Biol 17, 1272-1274.

Itkonen, H.M., Gorad, S.S., Duveau, D.Y., Martin, S.E., Barkovskaya, A., Bathen, T.F., Moestue, S.A., and Mills, I.G. (2016). Inhibition of O-GlcNAc transferase activity reprograms prostate cancer cell metabolism. Oncotarget 7, 12464-12476.

Joazeiro, C.A., and Weissman, A.M. (2000). RING finger proteins: mediators of ubiquitin ligase activity. Cell 102, 549-552.

Krzeslak, A., Forma, E., Bernaciak, M., Romanowicz, H., and Brys, M. (2012). Gene expression of O-GlcNAc cycling enzymes in human breast

cancers. Clin Exp Med 12, 61-65.

Love, D.C., and Hanover, J.A. (2005). The hexosamine signaling pathway: deciphering the "O-GlcNAc code". Sci STKE 2005, re13.

Lynch, T.P., Ferrer, C.M., Jackson, S.R., Shahriari, K.S., Vosseller, K., and Reginato, M.J. (2012). Critical role of O-Linked beta-N-acetylglucosamine transferase in prostate cancer invasion, angiogenesis, and metastasis. J Biol Chem 287, 11070-11081.

Lynch, T.P., and Reginato, M.J. (2011). O-GlcNAc transferase: a sweet new cancer target. Cell Cycle 10, 1712-1713.

Ma, Z., Vocadlo, D.J., and Vosseller, K. (2013). Hyper-O-GlcNAcylation is anti-apoptotic and maintains constitutive NF-kappaB activity in pancreatic cancer cells. J Biol Chem 288, 15121-15130.

Mi, W., Gu, Y., Han, C., Liu, H., Fan, Q., Zhang, X., Cong, Q., and Yu, W. (2011). O-GlcNAcylation is a novel regulator of lung and colon cancer malignancy. Biochim Biophys Acta 1812, 514-519.

Ozcan, S., Andrali, S.S., and Cantrell, J.E. (2010). Modulation of transcription factor function by O-GlcNAc modification. Biochim Biophys Acta 1799, 353-364.

Peacock, O., Lee, A.C., Cameron, F., Tarbox, R., Vafadar-Isfahani, N., Tufarelli, C., and Lund, J.N. (2014). Inflammation and MiR-21 pathways functionally interact to downregulate PDCD4 in colorectal cancer. PLoS One 9, e110267.

Roos, M.D., Su, K., Baker, J.R., and Kudlow, J.E. (1997). O glycosylation of an Sp1-derived peptide blocks known Sp1 protein interactions. Mol Cell Biol 17, 6472-6480.

Rozanski, W., Krzeslak, A., Forma, E., Brys, M., Blewniewski, M.,

Wozniak, P., and Lipinski, M. (2012). Prediction of bladder cancer based on urinary content of MGEA5 and OGT mRNA level. Clin Lab 58, 579-583.

Ruan, H.B., Nie, Y., and Yang, X. (2013). Regulation of protein degradation by O-GlcNAcylation: crosstalk with ubiquitination. Mol Cell Proteomics 12, 3489-3497.

Schimmer, A.D., Dalili, S., Batey, R.A., and Riedl, S.J. (2006). Targeting XIAP for the treatment of malignancy. Cell Death Differ 13, 179-188.

Seo, H.G., Kim, H.B., Kang, M.J., Ryum, J.H., Yi, E.C., and Cho, J.W. (2016). Identification of the nuclear localisation signal of O-GlcNAc transferase and its nuclear import regulation. Sci Rep 6, 34614.

Slawson, C., and Hart, G.W. (2011). O-GlcNAc signalling: implications for cancer cell biology. Nat Rev Cancer 11, 678-684.

Slawson, C., Housley, M.P., and Hart, G.W. (2006). O-GlcNAc cycling: how a single sugar post-translational modification is changing the way we think about signaling networks. J Cell Biochem 97, 71-83.

Srinivasula, S.M., and Ashwell, J.D. (2008). IAPs: what's in a name? Mol Cell 30, 123-135.

Suzuki, Y., Nakabayashi, Y., and Takahashi, R. (2001). Ubiquitin-protein ligase activity of X-linked inhibitor of apoptosis protein promotes proteasomal degradation of caspase-3 and enhances its anti-apoptotic effect in Fas-induced cell death. Proc Natl Acad Sci U S A 98, 8662-8667.

Wells, L., Vosseller, K., and Hart, G.W. (2001). Glycosylation of nucleocytoplasmic proteins: signal transduction and O-GlcNAc. Science 291, 2376-2378.

Wells, L., Whelan, S.A., and Hart, G.W. (2003). O-GlcNAc: a regulatory post-translational modification. Biochem Biophys Res Commun 302, 435-441.

Yang, X.K., Xing, H., Zheng, F., Gao, Q.L., Wang, W., Lu, Y.P., and Ma, D. (2003). [Role of apoptosis-associated genes and caspase-3 in cisplatin-resistant human ovarian cancer cell lines]. Zhonghua Fu Chan Ke Za Zhi 38, 158-161.

Zachara, N.E., and Hart, G.W. (2004). O-GlcNAc modification: a nutritional sensor that modulates proteasome function. Trends Cell Biol 14, 218-221.

Appendix

Site Mapping for *O*-GlcNAc Modification of X-linked Inhibitor of Apoptosis Protein (XIAP)

A

#1	c+	c+1+	Seq.	y+	z+	z+1+	z+1 2+	#2
1	119.08151	120.08933	T					18
2	266.14993	267.15775	F	1911.94476	1895.92604	1896.93387	948.97057	17
3	337.18705	338.19487	A	1764.87634	1748.85762	1749.86545	875.43636	16
4	451.22998	452.23780	N	1693.83922	1677.82050	1678.82833	839.91780	15
5	598.29840	599.30622	F	1579.79629	1563.77757	1564.78540	782.89634	14
6	695.35117	696.35899	P	1432.72787	1416.70915	1417.71698	709.36213	13
7	782.38320	783.39102	S	1335.67510	1319.65638	1320.66421	660.83574	12
8	839.40467	840.41249	G	1248.64307	1232.62435	1233.63218	617.31973	11
9	926.43670	927.44452	S	1191.62160	1175.60288	1176.61071	588.80899	10
10	1023.48947	1024.49729	P	1104.58957	1088.57085	1089.57868	545.29298	9
11	1122.55789	1123.56571	V	1007.53680	991.51808	992.52591	496.76659	8
12	1412.66929	1413.67711	S-HexNAc	908.46838	892.44966	893.45749	447.23238	7
13	1483.70641	1484.71423	A	618.35698	602.33826	603.34608	302.17668	6
14	1570.73844	1571.74626	S	547.31986	531.30114	532.30896	266.65812	5
15	1671.78612	1672.79394	T	460.28783	444.26911	445.27693	223.14210	4
16	1784.87019	1785.87801	L	359.24015	343.22143	344.22925	172.61826	3
17	1855.90731	1856.91513	A	246.15608	230.13736	231.14518	116.07623	2
18			R	175.11896	159.10024	160.10806	80.55767	1

B

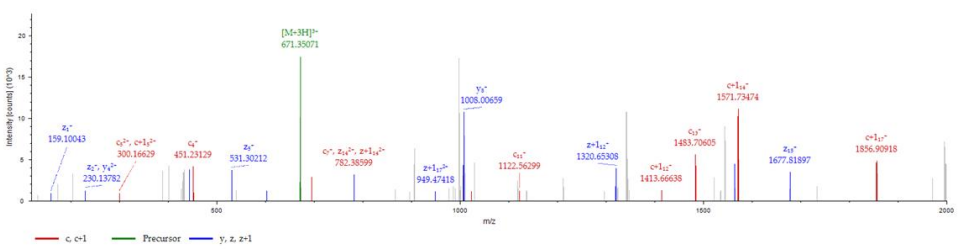

Figure 1. *O*-GlcNAc Position: Serine (43)

Sequence: TFANFPSGSPVSASTLAR, S12-HexNAc (203.07937 Da)

Charge: +3, Monoisotopic m/z: 671.66968 Da (+0.68 mmu/+1.01 ppm), MH+: 2012.99448 Da, RT: 39.82 min,

Identified with: Sequest HT (v1.3); XCorr:2.52, Fragment match tolerance used for search: 0.8 Da

A

#1	c+	c+1+	Seq.	y+	z+	z+1+	z+1²+	#2
1	119.08151	120.08933	T					18
2	266.14993	267.15775	F	1911.94476	1895.92604	1896.93387	948.97057	17
3	337.18705	338.19487	A	1764.87634	1748.85762	1749.86545	875.43636	16
4	451.22998	452.23780	N	1693.83922	1677.82050	1678.82833	839.91780	15
5	598.29840	599.30622	F	1579.79629	1563.77757	1564.78540	782.89634	14
6	695.35117	696.35899	P	1432.72787	1416.70915	1417.71698	709.36213	13
7	782.38320	783.39102	S	1335.67510	1319.65638	1320.66421	660.83574	12
8	839.40467	840.41249	G	1248.64307	1232.62435	1233.63218	617.31973	11
9	926.43670	927.44452	S	1191.62160	1175.60288	1176.61071	588.80899	10
10	1023.48947	1024.49729	P	1104.58957	1088.57085	1089.57868	545.29298	9
11	1122.55789	1123.56571	V	1007.53680	991.51808	992.52591	496.76659	8
12	1412.66929	1413.67711	S-HexNAc	908.46838	892.44966	893.45749	447.23238	7
13	1483.70641	1484.71423	A	618.35698	602.33826	603.34608	302.17668	6
14	1570.73844	1571.74626	S	547.31986	531.30114	532.30896	266.65812	5
15	1671.78612	1672.79394	T	460.28783	444.26911	445.27693	223.14210	4
16	1784.87019	1785.87801	L	359.24015	343.22143	344.22925	172.61826	3
17	1855.90731	1856.91513	A	246.15608	230.13736	231.14518	116.07623	2
18			R	175.11896	159.10024	160.10806	80.55767	1

B

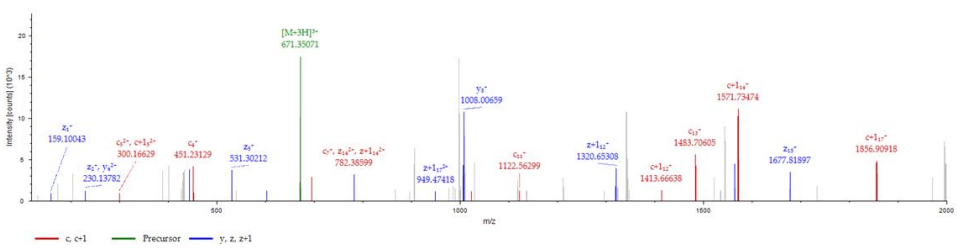

Figure 2. *O*-GlcNAc Position: Threonie (135)

Sequence: DHFALDRPSETHADYLLR, T11-HexNAc (203.07937 Da)

Charge: +4, Monoisotopic m/z: 590.53906 Da (+0.76 mmu/+1.28 ppm), MH+: 2359.13442 Da, RT: 41.92 min,

Identified with: Sequest HT (v1.3); XCorr:2.45, Fragment match tolerance used for search: 0.8 Da

A

#1	c+	c+1+	Seq.	y2+	z+	z+1+	z+12+	#2
1	132.07676	133.08458	N					15
2	245.16083	246.16865	L	876.42398	1735.82196	1736.82979	868.91853	14
3	359.20376	360.21158	N	819.88195	1622.73789	1623.74572	812.37650	13
4	472.28783	473.29565	I	762.86048	1508.69496	1509.70279	755.35503	12
5	628.38895	629.39677	R	706.31845	1395.61089	1396.61872	698.81300	11
6	918.50035	919.50817	S-HexNAc	628.26789	1239.50977	1240.51760	620.76244	10
7	1047.54295	1048.55077	E	483.21218	949.39837	950.40619	475.70673	9
8	1134.57498	1135.58280	S	418.69088	820.35577	821.36359	411.18543	8
9	1249.60193	1250.60975	D	375.17487	733.32374	734.33156	367.66942	7
10	1320.63905	1321.64687	A	317.66139	618.29679	619.30461	310.15594	6
11	1419.70747	1420.71529	V	282.14283	547.25967	548.26749	274.63738	5
12	1506.73950	1507.74732	S	232.60862	448.19125	449.19907	225.10317	4
13	1593.77153	1594.77935	S	189.09261	361.15922	362.16704	181.58716	3
14	1708.79848	1709.80630	D	145.57659	274.12719	275.13501	138.07114	2
15			R	88.06312	159.10024	160.10806	80.55767	1

B

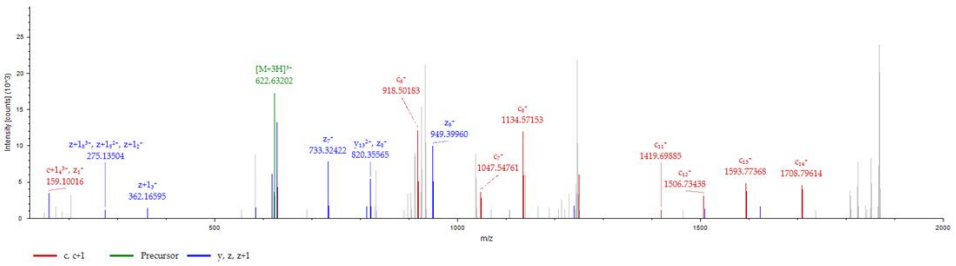

Figure 3. *O*-GlcNAc Position: Serine (239)

Sequence: NLNIRSESDAVSSDR, S6-HexNAc (203.07937 Da)

Charge: +3, Monoisotopic m/z: 622.63257 Da (-0.15 mmu/-0.25 ppm), MH+: 1865.88315 Da, RT: 19.99 min,

Identified with: Sequest HT (v1.3); XCorr:3.04,

Fragment match tolerance used for search: 0.8 Da

A

#1	b+	Seq.	y+	y2+	#2
1	88.03931	S			10
2	217.08191	E	1168.49646	584.75187	9
3	304.11394	S	1039.45386	520.23057	8
4	419.14089	D	952.42183	476.71456	7
5	490.17801	A	837.39488	419.20108	6
6	589.24643	V	766.35776	383.68252	5
7	879.35783	S-HexNAc	667.28934	334.14831	4
8	966.38986	S	377.17794	189.09261	3
9	1081.41681	D	290.14591	145.57659	2
10		R	175.11896	88.06312	1

B

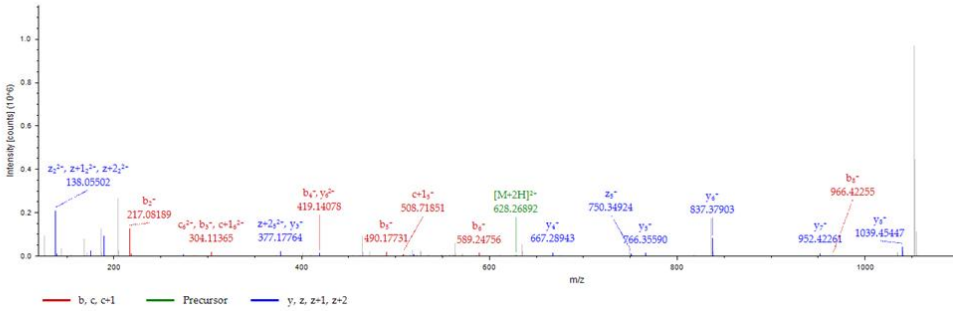

Figure 4. *O*-GlcNAc Position: Serine (245)

Sequence: SESDAVSSDR, S7-HexNAc (203.07937 Da)

Charge: +2, Monoisotopic m/z: 628.26770 Da (-0.19 mmu/-0.3 ppm), MH+: 1255.52812 Da, RT: 6.87 min,

Identified with: Sequest HT (v1.3); XCorr:1.60, Fragment match tolerance used for search: 0.8 Da

국문요약

O-GlcNAc Transferase의 핵 이동 신호 동정과 핵으로의 이동 기작 연구

연세대학교 대학원
융합오믹스 의생명과학과
서현규

세포 내 포도당, 글루타민, 아세틸코에이와 같은 영양물질의 상태에 따라 Hexosamine biosynthetic pathway (HBP)에 의한 신호전달이 일어나고, 증가된 HBP 신호전달은 핵과 세포질에 존재하는 단백질들의 *N*-acetylglucosamine을 전달하는 *O*-GlcNAc 수식화의 증가를 유도하게 된다. *O*-GlcNAc 수식화는 단백질들의 세린 또는 트레오닌 잔기에 *N*-acetylglucosamine이 *O*-linkage로 결합하는 것으로서, *O*-GlcNAc을 전달하는 효소인 *O*-GlcNAc transferase (OGT) 그리고 *O*-GlcNAc을 제거하는 효소인 *O*-GlcNAcase (OGA)에 의해 조절이 이루어진다.

OGT는 핵과 세포질에 존재하는 효소이며 OGT가 세포 내 핵 또는 세포질에 존재함에 따라 다양한 *O*-GlcNAc 수식화 기질 단백질 군이 변하게 되고 세포 내 신호 전달에 영향을 주게 되기 때문에 세포 내 OGT의 위치 결정은 매우 중요하다. 하지만 현재까지 OGT가 핵으로 유입 또는 유출되는 기작은 보고되어 있지 않다. 본 연구에서는 OGT에 존재하는 세 개의 아미노산으로 이루어진 새로운 핵 이동 서열 (DFP)을 동정하였으며 OGT의 수송 단백질로서 importin α5가 역할을 한다는 사실 또한 증명하였다. 이후에는 질량분석법을 통하여 OGT의 tetratricopeptide repeats (TPRs) 안에 존재하는 세린 389 위치의 *O*-GlcNAc 수식화 위치를 동정하였다. 세린 389 위치를 알라닌으로 치환한 돌연변이체를 이용한 연구를 통하여 세린 389의 *O*-GlcNAc 수식화 위치는 직접적으로 OGT의 핵으로 이동에 영

향을 준다는 사실을 증명하였다.

암세포에서는 특이적으로 OGT 단백질의 발현과 *O*-GlcNAc 수식화가 증가되어 있음이 관찰되어져 왔다. 많은 연구들이 이렇게 증가된 OGT 단백질과 *O*-GlcNAc 수식화가 암세포의 성장 및 전이 등의 특징을 갖게 하는데 중요함을 밝히었다. 하지만 OGT 단백질의 비정상적인 발현 유지가 중요함에도 불구하고 어떤 기작에 의해 OGT 단백질이 유지될 수 있는지에 대한 연구는 미비하였다. 본 연구에서는 X-linked inhibitor of apoptosis protein (XIAP)가 OGT와 상호작용하여 OGT를 기질단백질로 하여 유비퀴틴화를 일으키고 결과적으로 프로테아좀에 의해 분해가 유도됨을 밝히었다. XIAP 또한 *O*-GlcNAc 수식화가 일어나며 세린 406 위치에 일어나는 *O*-GlcNAc 수식화는 XIAP가 OGT에 대한 유비퀴틴화에 영향을 주는 기능을 하는 것을 증명하였다. 마지막으로 암 세포내 과발현된 XIAP는 OGT 단백질의 양을 줄임으로서 암세포의 성장을 저해한다는 사실을 밝히었다. 이와 같은 연구는 XIAP의 세포사멸 저해 인자로서의 본래 기능을 넘어서 암의 성장을 조절할 수 있는 새로운 기능을 제시하였다.

Key words: *O*-GlcNAc, *O*-GlcNAc transferase (OGT), 핵 이동 서열, importin α5, tetratricopeptide repaeats (TPR), 암세포, X-linked inhibitor apoptosis protein (XIAP), 유비퀴틴화, 프로테아좀, 세포사멸